Chapter 2
Basic Principles of SAR Polarimetry

The field of synthetic aperture radar changed dramatically in the early 1980s with the introduction of advance radar techniques, such as polarimetry and interferometry. While both of these techniques had been demonstrated much earlier, radar polarimetry only became an operational research tool with the introduction of the NASA/JPL Airborne Synthetic Aperture Radar (AIRSAR) system in the early 1980s. Radar polarimetry was proven from space with the two Spaceborne Imaging Radar C-band and X-band (SIR-C/X) SAR flights on board the space shuttle Endeavour in April and October 1994. In this chapter, we describe the basic principles of SAR polarimetry and, thereby, provide tools necessary to understand SAR polarimetry applications, such as land classification.

2.1 Polarization of Electromagnetic Waves

In SAR polarimetry, information is transmitted from an object to a sensor by electromagnetic waves. The information could be encoded in the frequency content, intensity, or polarization of the electromagnetic wave. The electromagnetic waves propagate at the velocity of light from the object directly through free space or indirectly by reflection, scattering, and radiation to the sensor. The interaction of electromagnetic waves with natural surfaces and atmospheres is strongly dependent on the frequency of the waves.

An electromagnetic wave consists of a coupled electric and magnetic force field. In free space, these two fields are at right angles to each other and transverse to the direction of propagation. The direction and magnitude of only one of the fields (usually the electric field) is sufficient to completely specify the direction and magnitude of the other field in free space using Maxwell's equations. The polarization of the electromagnetic wave is contained in the

elements of the vector amplitude $\mathbf{A}$ of the electric field. For a transverse electromagnetic wave, this vector is orthogonal to the direction in which the wave is propagating; we can, therefore, completely describe the amplitude of the electric field by writing $\mathbf{A}$ as a two-dimensional complex vector:

$$\mathbf{A} = a_h e^{i\delta_h}\hat{\mathbf{h}} + a_v e^{i\delta_v}\hat{\mathbf{v}}\,. \tag{2.1-1}$$

Here, we denote the two orthogonal basis vectors as $\hat{\mathbf{h}}$ for horizontal and $\hat{\mathbf{v}}$ for vertical. Horizontal polarization is usually defined as the state where the electric vector is perpendicular to the plane of incidence. Vertical polarization is orthogonal to both horizontal polarization and the direction of propagation and corresponds to the case where the electric vector is in the plane of incidence. Any two orthogonal basis vectors could be used to describe the polarization; in some cases, the right- and left-handed circular basis is used. The amplitudes, a_h and a_v, and the relative phases, δ_h and δ_v, are real numbers. The polarization of the wave can be thought of as the shape that the tip of the electric field would trace over time at a fixed point in space. Taking the real part of Eq. (2.1-1), we find that the polarization figure is the locus of all the points in the h-v plane that have the coordinates $E_h = a_h \cos\delta_h;\quad E_v = a_v \cos\delta_v$. It can easily be shown that the points on the locus satisfy the expression

$$\left(\frac{E_h}{a_h}\right)^2 + \left(\frac{E_v}{a_v}\right)^2 - 2\frac{E_h}{a_h}\frac{E_v}{a_v}\cos\left(\delta_h - \delta_v\right) = \sin^2\left(\delta_h - \delta_v\right). \tag{2.1-2}$$

This is the expression of an ellipse (shown in Fig. 2-1). In the general case, therefore, electromagnetic waves are elliptically polarized. In tracing the ellipse, the tip of the electric field can rotate either clockwise or counter-clockwise; this direction is denoted by the handedness of the polarization. The definition of handedness accepted by the Institute for Electrical and Electronics Engineers (IEEE) is that a wave is said to have right-handed polarization if the tip of the electric field vector rotates clockwise when the wave is viewed receding from the observer. If the tip of the electric field vector rotates counter-clockwise when the wave is viewed in the same way, it has a left-handed polarization. It is worth pointing out that a different definition of handedness is often encountered in optics literature. Specifically, in optics literature, a wave is said to have a right-handed (left-handed) polarization when the wave is viewed approaching the observer and the tip of the electric field vector rotates in the clockwise (counter-clockwise) direction.

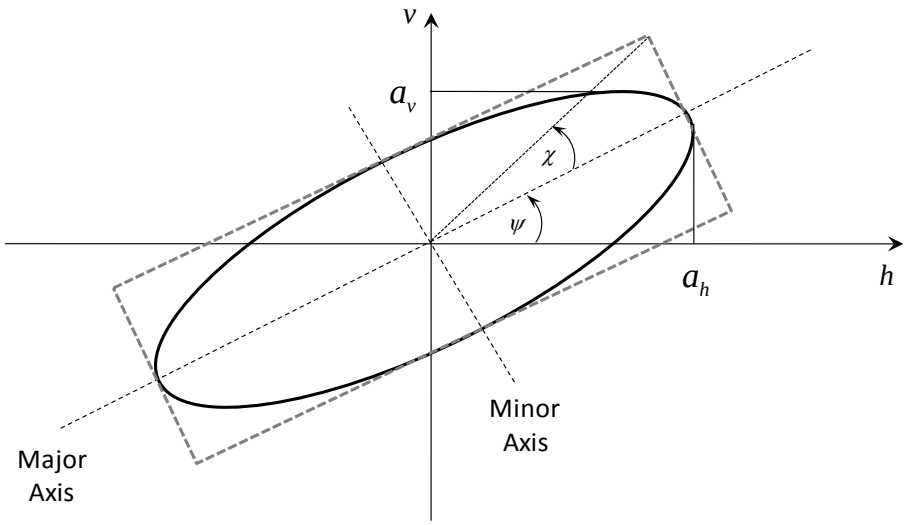

Fig. 2-1. A polarization ellipse.

In the special case where the ellipse collapses to a line, which happens when $\delta_h - \delta_v = n\pi$ with n any integer, the wave is said to be linearly polarized. Another special case is encountered when the two amplitudes are the same $(a_h = a_v)$ and the relative phase difference $\delta_h - \delta_v$ is either $\pi/2$ or $-\pi/2$. In this case, the wave is circularly polarized.

The polarization ellipse (see Fig. 2-1) can also be characterized by two angles known as the ellipse orientation angle (ψ in Fig. 2-1, $0 \le \psi \le \pi$) and the ellipticity angle, shown as χ ($-\pi/4 \le \chi \le \pi/4$) in Fig. 2-1. These angles can be calculated as follows:

$$\tan 2\psi = \frac{2a_h a_v}{a_h^2 - a_v^2}\cos(\delta_h - \delta_v); \quad \sin 2\chi = \frac{2a_h a_v}{a_h^2 + a_v^2}\sin(\delta_h - \delta_v). \qquad (2.1\text{-}3)$$

Note that linear polarizations are characterized by an ellipticity angle $\chi = 0$. Note also that two waves are orthogonally polarized: that is, the scalar product of the two polarization vectors will be zero if the two polarization ellipses have orientation angles that are 90 degrees (deg) different and the handedness of the two waves are opposite.

So far, it was implied that the amplitudes and phases shown in Eq. (2.1-1) and Eq. (2.1-2) are constant in time. This might not always be the case. If these quantities vary with time, the tip of the electric field vector will not trace out a smooth ellipse. Instead, the figure will, in general, be a noisy version of an

ellipse that after some time might resemble an "average" ellipse. In this case, the wave is said to be partially polarized, and it can be considered that part of the energy has a deterministic polarization state. The radiation from some sources, such as the Sun, does not have any clearly defined polarization. The electric field assumes different directions at random as the wave is received. In this case, the wave is called randomly polarized or unpolarized. In the case of some man-made sources, such as lasers and radio/radar transmitters, the wave usually has a well-defined polarized state.

Another way to describe the polarization of a wave that is particularly appropriate for the case of partially polarized waves is through the use of the Stokes parameters of the wave. For a monochromatic wave, these four parameters are defined as

$$\begin{aligned} S_0 &= |a_h|^2 + |a_v|^2 \\ S_1 &= |a_h|^2 - |a_v|^2 \\ S_2 &= 2a_h a_v \cos(\delta_h - \delta_v) \\ S_2 &= 2a_h a_v \sin(\delta_h - \delta_v) \end{aligned} . \tag{2.1-4}$$

Note that for such a fully polarized wave, only three of the Stokes parameters are independent, since $S_0^2 = S_1^2 + S_2^2 + S_3^2$. Using the relations in Eq. (2.1-3) between the ellipse orientation and ellipticity angles and the wave amplitudes and relative phases, it can be shown that the Stokes parameters can also be written as

$$\begin{aligned} S_1 &= S_0 \cos 2\chi \cos 2\psi \\ S_2 &= S_0 \cos 2\chi \sin 2\psi \\ S_3 &= S_0 \sin 2\chi \end{aligned} . \tag{2.1-5}$$

If two ellipse orientations differ by 90 deg and the handedness of the ellipses are opposite (that is, the ellipticity angles are equal but of opposite sign), it follows from Eq. (2.1-5) that the Stokes parameters of two orthogonally polarized waves are the same magnitudes, but opposite in sign.

The relations in Eq. (2.1-5) lead to a simple geometric interpretation of polarization states. The Stokes parameters S_1, S_2 and S_3 can be regarded as the Cartesian coordinates of a point on a sphere, known as the Poincaré sphere, of radius S_0 (see Fig. 2-2). There is, therefore, a unique mapping between the position of a point in the surface of the sphere and a polarization state. Linear polarizations map to points on the equator of the Poincaré sphere, while the circular polarizations map to the poles. Orthogonal polarizations are anti-podal

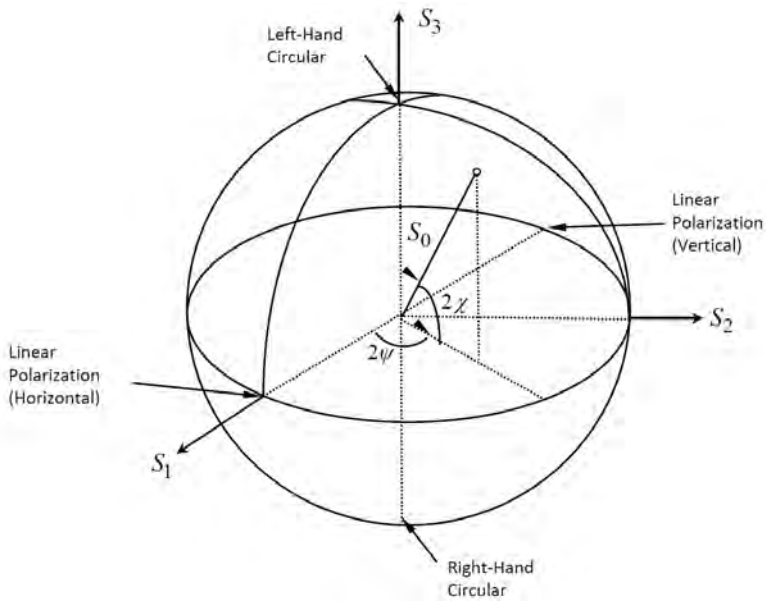

Fig. 2-2. Polarization represented as a point on the Poincaré sphere.

on the Poincaré sphere, which means they lie on opposite sides of the sphere and the line connecting the orthogonal polarizations runs through the center of the sphere. See, for example, the positions of horizontally and vertically polarized linear polarizations or the two circular polarizations in Fig. 2-2.

In the case of partially polarized waves, all four Stokes parameters are required to fully describe the polarization of the wave. In general, the Stokes parameters are related by $S_0^2 \geq S_1^2 + S_2^2 + S_3^2$, with equality holding only for fully polarized waves. In the extreme case of an unpolarized wave, the Stokes parameters are $S_0 > 0$ and $S_1 = S_2 = S_3 = 0$. It is always possible to describe a partially polarized wave by the sum of a fully polarized wave and an unpolarized wave. The magnitude of the polarized wave is given by $\sqrt{S_1^2 + S_2^2 + S_3^2}$; the magnitude of the unpolarized wave is $S_0 - \sqrt{S_1^2 + S_2^2 + S_3^2}$. Finally, it should be pointed out that the Stokes parameters of an unpolarized wave can be written as the sum of two fully polarized waves, as follows:

$$\begin{pmatrix} S_0 \\ 0 \\ 0 \\ 0 \end{pmatrix} = \frac{1}{2}\begin{pmatrix} S_0 \\ S_1 \\ S_2 \\ S_3 \end{pmatrix} + \frac{1}{2}\begin{pmatrix} S_0 \\ -S_1 \\ -S_2 \\ -S_3 \end{pmatrix}. \tag{2.1-6}$$

These two fully polarized waves have orthogonal polarizations. This important result shows that when an antenna with a particular polarization is used to receive unpolarized radiation, the amount of power received by the antenna will be only that half of the power in the unpolarized wave that aligns with the antenna polarization. The other half of the power will not be absorbed because its polarization is orthogonal to that of the antenna.

2.2 Mathematical Representations of Scatterers

If a radiated electromagnetic wave is scattered by an object and one observes this wave in the far-field of the scatterer, the scattered wave can, again, be adequately described by a two-dimensional vector. In this abstract way, one can consider the scatterer as a mathematical operator that takes one two-dimensional complex vector (the wave impinging upon the object) and changes that into another two-dimensional vector (the scattered wave). Mathematically, therefore, a scatterer can be characterized by a complex 2 × 2 scattering matrix:

$$\mathbf{E}^{sc} = \begin{pmatrix} S_{hh} & S_{hv} \\ S_{vh} & S_{vv} \end{pmatrix}\mathbf{E}^{tr} = [\mathbf{S}]\mathbf{E}^{tr} \tag{2.2-1}$$

where $\mathbf{E}^{tr}$ is the electric field vector that was transmitted by the radar antenna, $[\mathbf{S}]$ is the 2 × 2 complex scattering matrix that describes how the scatterer modified the incident electric field vector, and $\mathbf{E}^{sc}$ is the electric field vector that is incident on the radar receiving antenna. This scattering matrix is also a function of the radar frequency and the viewing geometry. The scatterer can, therefore, be thought of as a polarization transformer, with the transformation given by the scattering matrix. Once the complete scattering matrix is known and calibrated, one can synthesize the radar cross-section for any arbitrary combination of transmit and receive polarizations.

Fig. 2-3 shows a number of such synthesized images for the San Francisco Bay area in California. The data were acquired with the NASA/JPL AIRSAR system.

(a) Horizontal and vertical transmission

Fig. 2-3. This series of L-band images of San Francisco were synthesized from a single polarimetric image acquired by the NASA/JPL AIRSAR system at L-band. The nine images show the co-polarized (transmit and receive polarizations are the same) and the cross-polarized (transmit and receive polarizations are orthogonal) images for the three axes of the Poincaré sphere. They are (a)horizontal and vertical transmission, (b) different linear polarization angles, and (c) different circular polarizations. Note the relative change in brightness between the city of San Francisco, the ocean, and the Golden Gate Park, which is the large rectangle about 1/3 from the bottom of the images. The radar illumination is from the left.

(b) Different linear polarization angles

Fig. 2-3. This series of L-band images of San Francisco were synthesized from a single polarimetric image acquired by the NASA/JPL AIRSAR system at L-band. The nine images show the co-polarized (transmit and receive polarizations are the same) and the cross-polarized (transmit and receive polarizations are orthogonal) images for the three axes of the Poincaré sphere. They are (a)horizontal and vertical transmission, (b) different linear polarization angles, and (c) different circular polarizations. Note the relative change in brightness between the city of San Francisco, the ocean, and the Golden Gate Park, which is the large rectangle about 1/3 from the bottom of the images. The radar illumination is from the left.

(c) Different circular polarizations

Fig. 2-3. This series of L-band images of San Francisco were synthesized from a single polarimetric image acquired by the NASA/JPL AIRSAR system at L-band. The nine images show the co-polarized (transmit and receive polarizations are the same) and the cross-polarized (transmit and receive polarizations are orthogonal) images for the three axes of the Poincaré sphere. They are (a)horizontal and vertical transmission, (b) different linear polarization angles, and (c) different circular polarizations. Note the relative change in brightness between the city of San Francisco, the ocean, and the Golden Gate Park, which is the large rectangle about 1/3 from the bottom of the images. The radar illumination is from the left.

To specify the polarization vectors and electric field vectors, we need to define the radar coordinate system. In this book, we will use the backscatter alignment coordinate system as shown in Fig. 2-4; this is the coordinate system in which radar measurements are performed. (See Ulaby and Elachi, [1], Chapter 2, for a more detailed discussion of coordinate systems.)

The voltage measured by the radar system is proportional to the scalar product of the radar antenna polarization and the incident wave electric field, i.e.:

$$V = c_a \mathbf{p}^{rec} \cdot [\mathbf{S}] \mathbf{p}^{tr} , \tag{2.2-2}$$

where $\mathbf{p}^{tr}$ and $\mathbf{p}^{rec}$ are the normalized polarization vectors describing the transmitting and receiving radar antennas expressed in the backscatter alignment coordinate system, and c_a is a factor that includes the transmitting antenna gain, the receiving antenna effective area and the distance to the scatterer (see the derivation of the radar equation in Chapter 1). For our purposes here, we are interested in the properties of the scatterer, so we shall

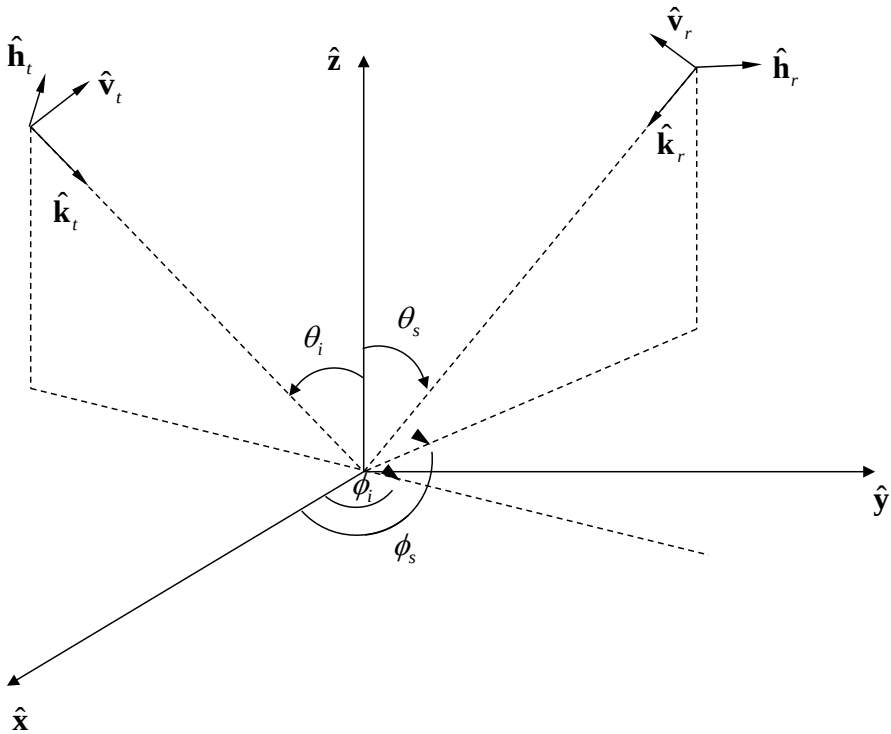

Fig. 2-4. A backscatter alignment coordinate system. Notice that the transmitting and receiving polarizations coincide for the backscattering case where the transmitting and receiving antennas are located at the same place.

ignore c_a in the rest of the discussion. The power received by the radar is the magnitude of the voltage squared (Kennaugh [2]; Kostinski and Boerner [3]; van Zyl et al. [4]; Zebker et al. [5]:

$$P = VV^* = \left|\mathbf{p}^{rec} \cdot [\mathbf{S}]\mathbf{p}^{tr}\right|^2. \tag{2.2-3}$$

Expanding the expression inside the magnitude sign in Eq. (2.2-3), it can be shown that the received power can also be written in terms of the scatterer covariance matrix, as follows:

$$P = VV^* = \left(\tilde{\mathbf{A}}\mathbf{T}\right)\left(\tilde{\mathbf{T}}\mathbf{A}\right)^* = \tilde{\mathbf{A}}\mathbf{T}\tilde{\mathbf{T}}^*\mathbf{A}^* = \mathbf{A}\cdot[\mathbf{C}]\mathbf{A}^*; \quad [\mathbf{C}] = \mathbf{T}\tilde{\mathbf{T}}^*, \tag{2.2-4}$$

where $\tilde{\mathbf{A}} = \begin{pmatrix} p_h^{rec} p_h^{tr} & p_h^{rec} p_v^{tr} & p_v^{rec} p_h^{tr} & p_v^{rec} p_v^{tr} \end{pmatrix}$ represents the transpose of the antenna polarization vector elements and $\tilde{\mathbf{T}} = \begin{pmatrix} S_{hh} & S_{hv} & S_{vh} & S_{vv} \end{pmatrix}$ represents only the scatterer. The superscript * denotes complex conjugation. The covariance matrix characterization is particularly useful when analyzing multi-look radar images, since the covariance matrix of a multi-look pixel is simply the average covariance matrix of all the individual measurements contained in the multi-look pixel.

Recall that multi-looking is performed by averaging the power from adjacent pixels together to reduce speckle. This averaging process can be written as

$$\langle P \rangle = \frac{1}{MN}\sum_{j=1}^{M}\sum_{i=1}^{N} P_{ij} = \frac{1}{MN}\sum_{j=1}^{M}\sum_{i=1}^{N} \mathbf{A}\cdot[C]_{ij}\,\mathbf{A}^* = \mathbf{A}\cdot\langle[\mathbf{C}]\rangle\mathbf{A}^*, \tag{2.2-5}$$

where the two subscripts denote averaging in the range and azimuth directions, respectively. The angular brackets $\langle\ \rangle$ denote this spatial averaging.

Eq. (2.2-4) shows the covariance matrix to be a 4 × 4 complex Hermetian matrix. In the case of radar backscatter, reciprocity dictates that $S_{hv} = S_{vh}$ and the covariance matrix can, in general, be written as a 3 × 3 complex Hermetian matrix. Also note that it is always possible to calculate the covariance matrix from the scattering matrix. However, the inverse is not true: it is not always possible to calculate an equivalent scattering matrix from the covariance matrix. This follows from the fact that the off-diagonal terms in the covariance matrix involve cross-products of the scattering matrix elements (for example, $S_{hh}S_{hv}^*$). For a single scattering matrix, there is a definite relationship between this term and the two diagonal terms $S_{hh}S_{hh}^*$ and $S_{hv}S_{hv}^*$. However, once the covariance

matrix elements are averaged spatially (such as during multi-looking of an image), this definite relationship no longer holds and we cannot uniquely find an equivalent S_{hh} and S_{hv} that would satisfy all three cross-products $\left\langle S_{hh}S_{hv}^{*}\right\rangle$, $\left\langle S_{hh}S_{hh}^{*}\right\rangle$, and $\left\langle S_{hv}S_{hv}^{*}\right\rangle$.

The power expression shown in Eq. (2.2-3) can also be written in terms of the antenna Stokes vectors. First, consider the following form of the power equation (van Zyl [6]; van Zyl et al. [7]):

$$\begin{aligned}
P &= \left(\mathbf{p}^{rec}\cdot\mathbf{E}^{sc}\right)\left(\mathbf{p}^{rec}\cdot\mathbf{E}^{sc}\right)^{*} \\
&= \left(p_h^{rec}E_h^{sc}+p_v^{rec}E_v^{sc}\right)\left(p_h^{rec}E_h^{sc}+p_v^{rec}E_v^{sc}\right)^{*} \\
&= \left(p_h^{rec}p_h^{rec*}\right)\left(E_h^{sc}E_h^{sc*}\right)+\left(p_v^{rec}p_v^{rec*}\right)\left(E_v^{sc}E_v^{sc*}\right) \\
&\quad +\left(p_h^{rec}p_v^{rec*}\right)\left(E_h^{sc}E_v^{sc*}\right)+\left(p_v^{rec}p_h^{rec*}\right)\left(E_v^{sc}E_h^{sc*}\right) \\
&= \begin{pmatrix} p_h^{rec}p_h^{rec*} \\ p_v^{rec}p_v^{rec*} \\ p_h^{rec}p_v^{rec*} \\ p_v^{rec}p_h^{rec*} \end{pmatrix}\cdot\begin{pmatrix} E_h^{sc}E_h^{sc*} \\ E_v^{sc}E_v^{sc*} \\ E_h^{sc}E_v^{sc*} \\ E_v^{sc}E_h^{sc*} \end{pmatrix} \\
&= \mathbf{g}^{rec}\cdot\mathbf{X}
\end{aligned} \tag{2.2-6}$$

Here, the vector $\mathbf{X}$ in Eq. (2.2-6) is a function of the transmit antenna parameters and the scattering matrix elements. Using the fact that $\mathbf{E}^{sc}=[\mathbf{S}]\mathbf{p}^{tr}$, it can be shown that $\mathbf{X}=[\mathbf{W}]\mathbf{g}^{tr}$, where

$$[\mathbf{W}]=\begin{pmatrix} S_{hh}S_{hh}^{*} & S_{hv}S_{hv}^{*} & S_{hh}S_{hv}^{*} & S_{hv}S_{hh}^{*} \\ S_{vh}S_{vh}^{*} & S_{vv}S_{vv}^{*} & S_{vh}S_{vv}^{*} & S_{vv}S_{vh}^{*} \\ S_{hh}S_{vh}^{*} & S_{hv}S_{vv}^{*} & S_{hh}S_{vv}^{*} & S_{hv}S_{vh}^{*} \\ S_{vh}S_{hh}^{*} & S_{vv}S_{hv}^{*} & S_{vh}S_{hv}^{*} & S_{vv}S_{hh}^{*} \end{pmatrix}. \tag{2.2-7}$$

Therefore, the measured power can be expressed as

$$P=\mathbf{g}^{rec}\cdot[\mathbf{W}]\mathbf{g}^{tr}. \tag{2.2-8}$$

The Stokes vector of a wave can be written as

$$\mathbf{S} = \begin{pmatrix} p_h p_h^* + p_v p_v^* \\ p_h p_h^* - p_v p_v^* \\ p_h p_v^* + p_h^* p_v \\ -i(p_h p_v^* - p_h^* p_v) \end{pmatrix} = \begin{pmatrix} 1 & 1 & 0 & 0 \\ 1 & -1 & 0 & 0 \\ 0 & 0 & 1 & 1 \\ 0 & 0 & -i & i \end{pmatrix} \begin{pmatrix} p_h p_h^* \\ p_v p_v^* \\ p_h p_v^* \\ p_h^* p_v \end{pmatrix} = [\mathbf{R}]\mathbf{g} \quad . \tag{2.2-9}$$

From Eq. (2.2-9), $\mathbf{g} = [\mathbf{R}]^{-1}\mathbf{S}$. Then, after straightforward calculations, it can be shown that

$$P = \mathbf{S}^{rec} \cdot [\mathbf{M}]\mathbf{S}^{tr} . \tag{2.2-10}$$

The matrix $[\mathbf{M}]$ is known as the Stokes scattering operator and is given by

$$[\mathbf{M}] = \left[[\mathbf{R}]^{-1}\right]^T [\mathbf{W}][\mathbf{R}]^{-1}, \tag{2.2-11}$$

where the superscript T indicates the transpose of the matrix. Note that, like the covariance matrix, the average power can be written in terms of the average Stokes scattering operator.

2.3 Implementation of a Radar Polarimeter

Polarimetric radars must measure the full scattering matrix to preserve the information regarding the scatterer. From Eq. (2.2-2), it can be seen that setting one transmit vector element equal to zero allows us to measure two components of the scattering matrix at a time. Mathematically, this operation is expressed as

$$\begin{pmatrix} S_{hh} \\ S_{vh} \end{pmatrix} = \begin{pmatrix} S_{hh} & S_{hv} \\ S_{vh} & S_{vv} \end{pmatrix} \begin{pmatrix} 1 \\ 0 \end{pmatrix}^{tr} ; \begin{pmatrix} S_{hv} \\ S_{vv} \end{pmatrix} = \begin{pmatrix} S_{hh} & S_{hv} \\ S_{vh} & S_{vv} \end{pmatrix} \begin{pmatrix} 0 \\ 1 \end{pmatrix}^{tr} . \tag{2.3-1}$$

Eq. (2.3-1) represents the typical implementation of a radar polarimeter: that is, a radar polarimeter transmits a wave of one polarization and receiving echoes in two orthogonal polarizations simultaneously. This is followed by transmitting a wave with a second polarization and, again, receiving echoes with both polarizations simultaneously (as is shown in Fig. 2-5). In this way, all four elements of the scattering matrix are measured. This implementation means that the transmitter is in slightly different positions when measuring the two columns of the scattering matrix, but this distance between the two positions is typically small compared to a synthetic aperture and, therefore, does not lead to a significant decorrelation of the signals. The more important aspect of this

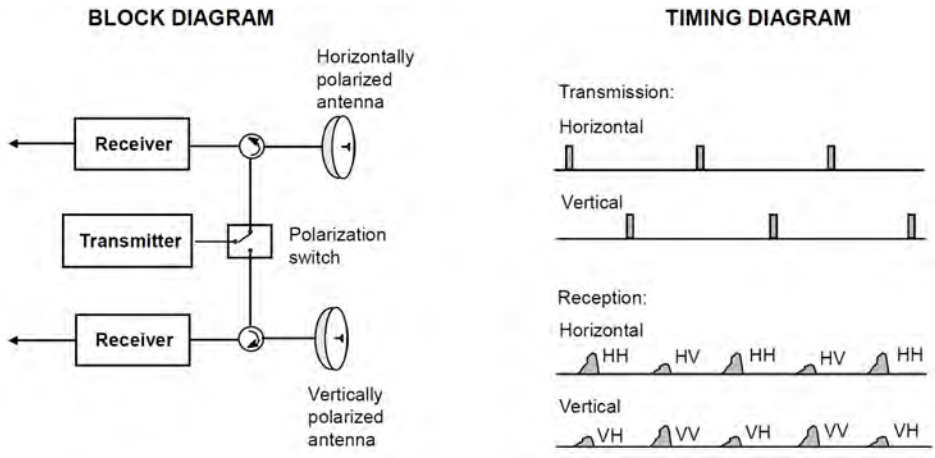

Fig. 2-5. A polarimetric radar is implemented by alternatively transmitting signals out of horizontally and vertically polarized antennas and receiving at both polarizations simultaneously. Two pulses are needed to measure all the elements in the scattering matrix.

implementation is that the pulse repetition frequency (PRF) must be high enough to ensure that each polarimetric channel is sampled adequately. Therefore, each channel must independently satisfy the minimum PRF requirement. Since we are interleaving two measurements, this means that the master PRF for a polarimetric system runs twice the rate of a single-channel SAR. The NASA/JPL AIRSAR system pioneered this implementation for SAR systems. Subsequently, the same implementation was used in the SIR-C part of the SIR-C/X-SAR radars.

A polarimetric SAR implemented in this fashion actually acquires four images: one each for the horizontal-horizontal (HH), horizontal-vertical (HV), vertical-horizontal (VH), and vertical-vertical (VV) combinations. The basic measurement for each pixel in the highest resolution image is, therefore, a complete scattering matrix, or four complex numbers. If the SAR operates in the backscatter mode, reciprocity dictates that $S_{hv} = S_{vh}$ and that there are only three independent images. In practice, the HV and VH measurements are made at different times and through different receivers, so thermal noise in the system will cause these numbers to be different. Once the channels are properly calibrated, any remaining differences are due to thermal noise. Therefore, one could, in fact, average these two channels together coherently to increase the signal-to-noise ratio in the cross-polarized image. After this operation, one is left with three independent complex numbers per pixel.

As discussed in the previous chapter, all SAR images suffer from speckle noise, which is the result of coherent interference from individual scatterers that might be present inside a pixel. To reduce this speckle noise, the power from adjacent

pixels are averaged; this process is known as multi-looking. We have shown in Eq. (2.2-5) that all the polarimetric information can be retained by performing this multi-looking operation by averaging the covariance matrices of adjacent pixels. A similar operation follows from Eq. (2.2-10) for the Stokes scattering operator case, as follows:

$$P_m = \langle P \rangle = \frac{1}{MN}\sum_{j=1}^{M}\sum_{i=1}^{N} P_{ij} = \frac{1}{MN}\sum_{j=1}^{M}\sum_{i=1}^{N} \mathbf{S}^{rec} \cdot [\mathbf{M}]_{ij}\, \mathbf{S}^{tr} = \mathbf{S}^{rec} \cdot \langle [\mathbf{M}] \rangle \mathbf{S}^{tr} \,. \tag{2.3-2}$$

This multi-looking operation can be done once; all subsequent analyses would then be performed on the multi-looked data set. In fact, the polarimetric data from the NASA/JPL AIRSAR system is distributed in a multi-looked format with some special compression formatting to reduce the data volume further. The multi-looked polarimetric data from the SIR-C radar was distributed as cross-products of the scattering matrix, which are the elements of the covariance matrix.

Polarimetric SAR systems place additional restrictions on the pulse repetition frequency (PRF) used to operate the radar. Each transmit polarization channel must satisfy the normal constraints imposed on SAR systems using a single transmit polarization. The result is that polarimetric systems operate with a master PRF that runs twice as fast as that of a single transmit channel SAR. Additionally, the range ambiguities of a polarimetric SAR system are more complicated than those of a single channel SAR. In the HV channel, for example, one would measure ambiguous signals from the next and the previous pulses (in fact, at all odd numbers of ambiguous pulses) at HH. Given that HV is usually much smaller than HH to begin with, we then have to place even more stringent requirements on the overall ambiguity levels to measure HV accurately in the presence of the ambiguities. This severely limits the useful swath width that can be achieved with polarimetric SAR systems from space.

One way to achieve much of the desirable information from a polarimetric measurement with reduced requirements on the PRF and the ambiguity level is to use so-called compact polarimetry (Souyris et al. [8]). Compact polarimetry essentially is a special, dual-polarization mode in which one polarization only is transmitted and two orthogonal polarizations are used to measure the return. In the original mode proposed by Souyris et al. [8], a 45 deg linear polarization signal is transmitted and horizontal and vertical polarizations are used to receive the signal. In this case, the received signal is simply

$$V_h = \frac{1}{\sqrt{2}}\left(S_{hh} + S_{hv}\right); \quad V_v = \frac{1}{\sqrt{2}}\left(S_{vh} + S_{vv}\right). \tag{2.3-3}$$

The average covariance matrix is then

$$\left\langle \left[C_p \right] \right\rangle \approx \frac{1}{2} \begin{pmatrix} \left\langle S_{hh} S_{hh}^* \right\rangle + \left\langle S_{hv} S_{hv}^* \right\rangle & \left\langle S_{hh} S_{vv}^* \right\rangle + \left\langle S_{hv} S_{hv}^* \right\rangle \\ \left\langle S_{vv} S_{hh}^* \right\rangle + \left\langle S_{hv} S_{hv}^* \right\rangle & \left\langle S_{hv} S_{hv}^* \right\rangle + \left\langle S_{vv} S_{vv}^* \right\rangle \end{pmatrix}. \tag{2.3-4}$$

In deriving this covariance matrix, we have assumed that the terrain exhibits reflection symmetry. Compact polarimetry allows us to relax the requirements on the PRF to be the same as that of a conventional SAR system. Compact polarimetry also balances the ambiguity levels better than that of a regular polarimetric system. The drawback, of course, is that we no longer have “pure” measurements of co-polarized and cross-polarized terms. Instead, we have mixtures of co- and cross-polarized terms in all components of the covariance matrix.

Following the original proposed compact polarimetry mode, Raney [9] suggested transmitting circular polarization to be more advantageous in the presence of Faraday rotation. The basic expressions are similar to those derived above, however, and will not be repeated here.

2.4 Polarization Response

Once the scattering matrix, the covariance matrix, or the Stokes matrix is known, one can synthesize the received power for any transmit and receive antenna polarizations using the power equations ((Eq. (2.2-3), Eq. (2.2-4), and Eq. (2.2-10)). This is known as polarization synthesis and is discussed in more detail in Chapter 2 of Ulaby and Elachi [1]. Note that if we allow the polarization of the transmit and receive antennas to be varied independently, the polarization response of the scene would be a four-dimensional space. This is most easily understood by representing each of the two polarizations by the orientation and ellipticity angles of the respective polarization ellipses. The polarization response is, therefore, a function of these four angles. Visualizing such a four-dimensional response is not easy. To simplify the visualization, the so-called polarization response (van Zyl [6]; Agrawal and Boerner [10]; Ulaby and Elachi [1]) was introduced. The polarization response is displayed as a three-dimensional figure, and the transmit and receive polarizations are either the same (the co-polarized response) or they are orthogonal (the cross-polarized response). One can also display the maximum or minimum received power as a function of transmit polarization or the polarized and unpolarized component of the power using this same display. Agrawal and Boerner [10] also used this method to display the relative phase of the received signal as a function of polarization.

We shall introduce the polarization response through the example of a trihedral corner reflector that has been used extensively for the polarimetric radar

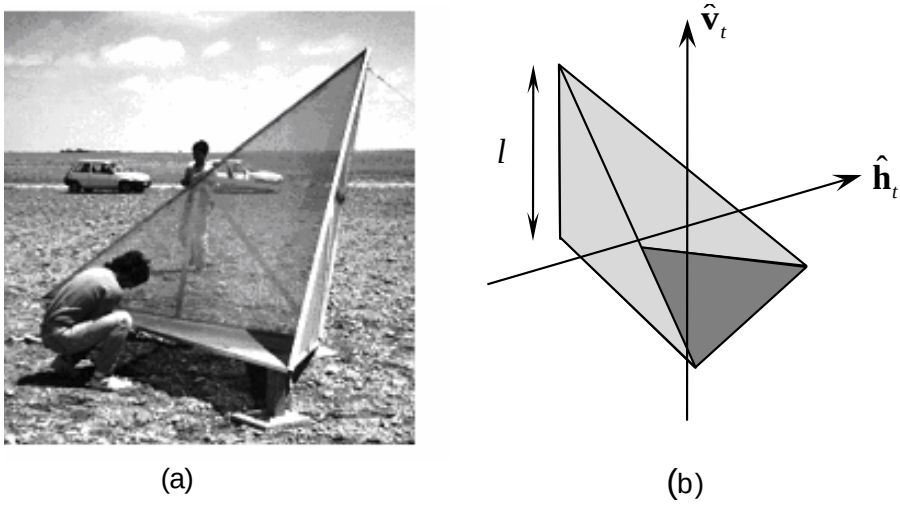

Fig. 2-6. (a) A trihedral corner reflector is being deployed at the calibration site. (b) The trihedral corner reflector geometry.

calibration. A picture of a trihedral corner reflector is shown in Fig. 2-6. The scattering matrix of a trihedral corner reflector is given by

$$[\mathbf{S}] = c_1 \begin{pmatrix} 1 & 0 \\ 0 & 1 \end{pmatrix}, \tag{2.4-1}$$

where $c_1 = \dfrac{k_0 l^2}{\sqrt{12}\pi}$. From Eq. (2.4-1), the characteristics of a trihedral corner reflector are:

1. No cross polarization components are generated (HV = VH = 0) for the linear polarization case.
2. Horizontal and vertical backscattering cross sections are identical (HH = VV).
3. Horizontal and vertical co-polarized components are in phase.

These are the desired properties of a calibration target to balance the co-polarized elements (i.e., the diagonal terms) of the scattering matrix. In addition, trihedral corner reflectors provide relatively large radar cross sections with a large, 3-dB beamwidth independent of the radar wavelength and the corner reflector size.

From Eq. (2.4-1), Eq. (2.2-4), and Eq. (2.2-11), we can calculate the covariance matrix and the Stokes scattering operator as

$$[\mathbf{C}] = |c_1|^2 \begin{pmatrix} 1 & 0 & 0 & 1 \\ 0 & 0 & 0 & 0 \\ 0 & 0 & 0 & 0 \\ 1 & 0 & 0 & 1 \end{pmatrix} \tag{2.4-2}$$

and

$$[\mathbf{M}] = \frac{1}{2}|c_1|^2 \begin{pmatrix} 1 & 0 & 0 & 0 \\ 0 & 1 & 0 & 0 \\ 0 & 0 & 1 & 0 \\ 0 & 0 & 0 & -1 \end{pmatrix}. \tag{2.4-3}$$

Using Eq. (2.2-10) and Eq. (2.4-3), the received power can be calculated explicitly, as shown in Eq. (2.4-4) for the case of co-polarized and cross-polarized antennas:

$$\begin{aligned} P &= \frac{k_0^2 l^4}{24\pi^2}\left\{1 \pm \cos^2(2\psi)\cos^2(2\chi) \pm \sin^2(2\psi)\cos^2(2\chi) \mp \sin^2(2\chi)\right\} \\ &= \frac{k_0^2 l^4}{24\pi^2}\left\{1 \pm \left[\cos^2(2\chi) - \sin^2(2\chi)\right]\right\} \\ &= \frac{k_0^2 l^4}{24\pi^2}\left\{1 \pm \cos(4\chi)\right\} \end{aligned}, \tag{2.4-4}$$

where the top sign is for the co-polarization case and the bottom sign is for the cross-polarization case. (Recall that orthogonally polarized waves are anti-podal on the Poincaré sphere.) The ellipse orientation and ellipticity angles refer to those of the transmitting antenna. It is immediately apparent that the received power is independent of the ellipticity angle. Taking the derivative with respect to the ellipse orientation angle, it is easily shown that for the co-polarized response, the maximum is found when $\chi = 0$ (linear polarizations) and the minimum occurs at $\chi = 45°$ (circular polarizations). The locations of the maxima and minima are reversed in the case of the cross-polarized response. This behavior is explained by the fact that the reflected waves have the opposite handedness than the transmitted ones when analyzed in the backscatter alignment coordinate system. Therefore, if either circular polarization is transmitted, the reflected wave is polarized orthogonally to the transmitted wave, leading to maximum reception in the cross-polarized and minimum reception in the co-polarized case.

The co- and cross-polarized responses are shown in Fig. 2-7. These three-dimensional displays show the normalized radar cross-section (power) in the vertical direction plotted as a function of the transmitting antenna ellipse orientation and ellipticity angles. For co-polarized responses, the receiving antenna has the same polarization as that of the transmitting antenna. The left-hand figure in Fig. 2-7 shows the positions of some of the more common antenna combinations for this type of display. For the cross-polarized response, the receiving antenna polarization is orthogonal to that of the transmitting antenna. Some of the common combinations are shown on the right in Fig. 2-7. Note that the displays in Fig. 2-7 confirm what we already discussed using Eq. (2.4-4). First, the received power is not a function of the ellipse orientation angle, as seen by the constant value of the radar cross-section in Fig. 2-7 for changing ellipse orientation. The maximum of the co-polarization signature occurs for the linear polarizations, and the minima at the circular polarizations. For the cross-polarization response, the maxima occur at the circular polarizations, while the minima occur at the linear polarizations.

A slightly different display of the polarization response involves displaying the normalized radar cross-section in spherical coordinates using the Poincaré sphere. The polarization is defined by the angles as shown in Fig. 2-2, but the radius is plotted as the normalized received power. This three-dimensional version of the polarization responses for the trihedral corner reflector is shown in Fig. 2-8. The co-polarized response clearly shows the nulls at the circular polarizations; the cross-polarized response shows the corresponding maximum for the circular polarizations.

The second example of polarization responses is that of a dihedral corner reflector, shown in Fig. 2-9. The scattering matrix of a dihedral corner reflector

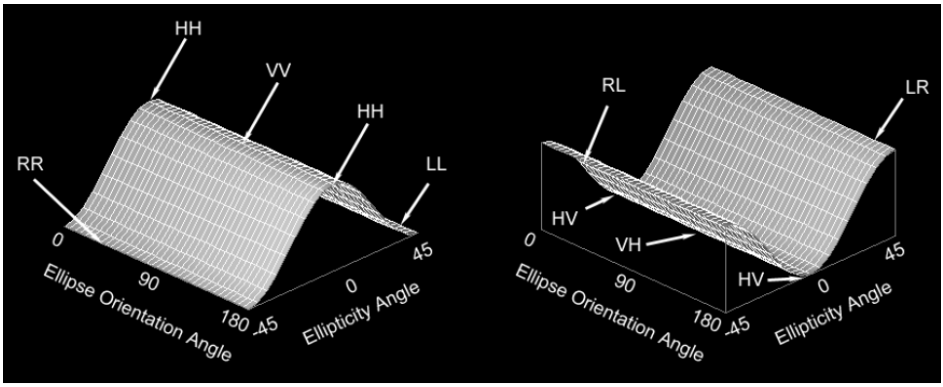

Fig. 2-7. The polarization response of a trihedral corner reflector. Two responses are displayed: (right) identical transmit and receive polarizations (co-polarized) and (left) orthogonal transmit and receive polarizations (cross-polarized).

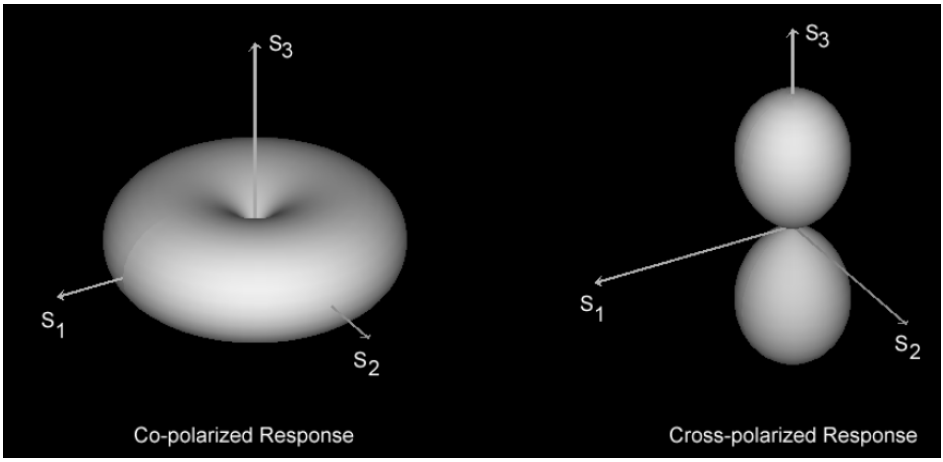

Fig. 2-8. Three-dimensional polarization response of a trihedral corner reflector.

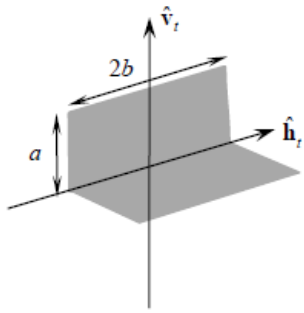

Fig. 2-9. A dihedral corner reflector.

is given by

$$[\mathbf{S}] = c_2 \begin{pmatrix} 1 & 0 \\ 0 & -1 \end{pmatrix}, \tag{2.4-5}$$

where $c_2 = \dfrac{k_0 ab}{\pi}$. From Eq. (2.4-5), we find the following characteristics for a dihedral corner reflector:

1. No cross polarization components are generated (HV = VH = 0) when it is illuminated by a purely horizontal or vertical radar signal.
2. Horizontal and vertical backscattering cross sections are identical (HH = VV).
3. Horizontal and vertical co-polarization components are out of phase.

From Eq. (2.4-5), we can calculate the covariance matrix and the Stokes scattering operator as

$$[\mathbf{C}] = |c_2|^2 \begin{pmatrix} 1 & 0 & 0 & -1 \\ 0 & 0 & 0 & 0 \\ 0 & 0 & 0 & 0 \\ -1 & 0 & 0 & 1 \end{pmatrix} \tag{2.4-6}$$

and

$$[\mathbf{M}] = \frac{1}{2}|c_2|^2 \begin{pmatrix} 1 & 0 & 0 & 0 \\ 0 & 1 & 0 & 0 \\ 0 & 0 & -1 & 0 \\ 0 & 0 & 0 & 1 \end{pmatrix}. \tag{2.4-7}$$

The received power from a dihedral corner reflector for the co- and cross-polarized cases can be written as

$$\begin{aligned} P &= \frac{k_0^2 a^2 b^2}{\pi^2}\left\{1 \pm \cos^2(2\psi)\cos^2(2\chi) \mp \sin^2(2\psi)\cos^2(2\chi) \pm \sin^2(2\chi)\right\} \\ &= \frac{k_0^2 a^2 b^2}{\pi^2}\left\{1 \pm \cos^2(2\chi)\cos(4\psi) \pm \sin^2(2\chi)\right\} \end{aligned}. \tag{2.4-8}$$

Taking the derivatives of this expression, one finds that the co-polarized maxima occur at horizontal linear, vertical linear, and the circular polarizations. The co-polarized minima occur at 45 deg and 135 deg linear polarizations. The cross-polarized maxima occur at the same polarizations as the co-polarized minima. The cross-polarized minima occur at the same polarizations as the co-polarized maxima. This information allows us to conclude that the minima observed in these responses occur because the polarization of the received wave is orthogonal to that of the transmitting antenna.

Figure 2-10 shows the co- and cross-polarized responses of the dihedral corner reflector. Note that the minima in one figure correspond to the maxima in the other. While not obvious when comparing Fig. 2-7 and the top row in Fig. 2-10, a comparison of Fig. 2-8 and the bottom row of Fig. 2-10 clearly shows that the polarization responses of the dihedral and trihedral corner reflectors are rotated versions of each other in the Poincaré space. In fact, the responses of the dihedral corner reflector are exactly those of the trihedral rotated 90 deg about the S_1 axis. In that sense, we can consider these responses as “orthogonal” to each other.

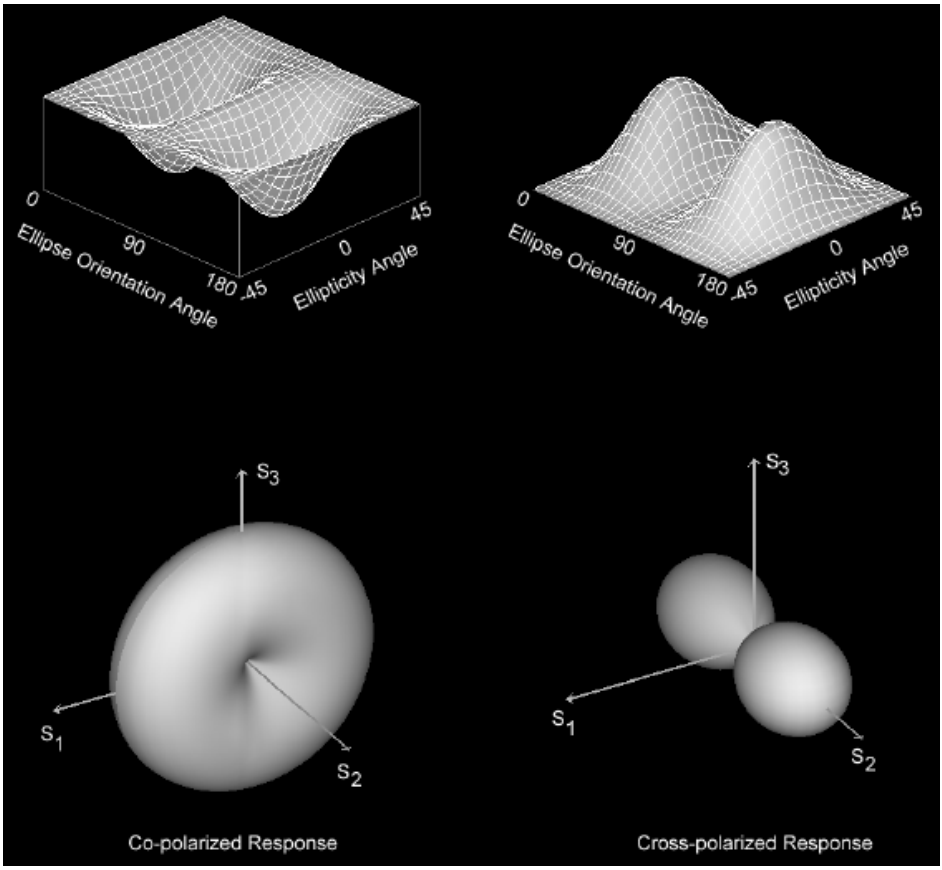

Fig. 2-10. Standard (top row) and three-dimensional (bottom row) polarization responses of a dihedral corner reflector.

Next, consider the case of a dihedral corner reflector, such as the one showed in Fig. 2-9; for this case, however, we rotate the base of the corner reflector 45 deg relative to the horizontal axis. Consequently, the scattering matrix becomes

$$[\mathbf{S}] = c_2 \begin{pmatrix} 0 & 1 \\ 1 & 0 \end{pmatrix}, \tag{2.4-9}$$

where $c_2 = \dfrac{k_0 ab}{\pi}$, as before. The covariance matrix and the Stokes scattering operator are

$$[\mathbf{C}] = |c_2|^2 \begin{pmatrix} 0 & 0 & 0 & 0 \\ 0 & 1 & 1 & 0 \\ 0 & 1 & 1 & 0 \\ 0 & 0 & 0 & 0 \end{pmatrix} \tag{2.4-10}$$

and

$$[\mathbf{M}] = \frac{1}{2}|c_3|^2 \begin{pmatrix} 1 & 0 & 0 & 0 \\ 0 & -1 & 0 & 0 \\ 0 & 0 & 1 & 0 \\ 0 & 0 & 0 & 1 \end{pmatrix}. \tag{2.4-11}$$

The received power from a rotated dihedral corner reflector for the co- and cross-polarized cases can be written as

$$\begin{aligned} P &= \frac{k_0^2 a^2 b^2}{\pi^2}\left\{1 \mp \cos^2(2\psi)\cos^2(2\chi) \pm \sin^2(2\psi)\cos^2(2\chi) \pm \sin^2(2\chi)\right\}. \\ &= \frac{k_0^2 a^2 b^2}{\pi^2}\left\{1 \mp \cos^2(2\chi)\cos(4\psi) \pm \sin^2(2\chi)\right\} \end{aligned} \tag{2.4-12}$$

The polarization responses for this rotated dihedral corner reflector are shown in Fig. 2-11. Note that the cross-polarized maxima are now at HV and VH, with corresponding zeros at HH and VV. The three-dimensional signature in Fig. 2-11 shows that the responses of this rotated dihedral are the same shape as those of the trihedral, but rotated by 90 deg about the S_2 axis. They are in some sense "orthogonal" to the responses of both the trihedral and the non-rotated dihedral.

The scattering from vegetation is often modeled using a combination of randomly oriented cylinders. For the short, thin, vertical-conducting cylinder shown in Fig. 2-12, the scattering matrix is given by

$$[\mathbf{S}] = c_3 \begin{pmatrix} 0 & 0 \\ 0 & 1 \end{pmatrix}, \tag{2.4-13}$$

where $c_3 = \dfrac{k_0^2 l^3}{6\left[\ln(4l/a) - 1\right]}$ and a is the radius of a cylinder.

From Eq. (2.4-13), we can calculate the covariance matrix and the Stokes scattering operator as

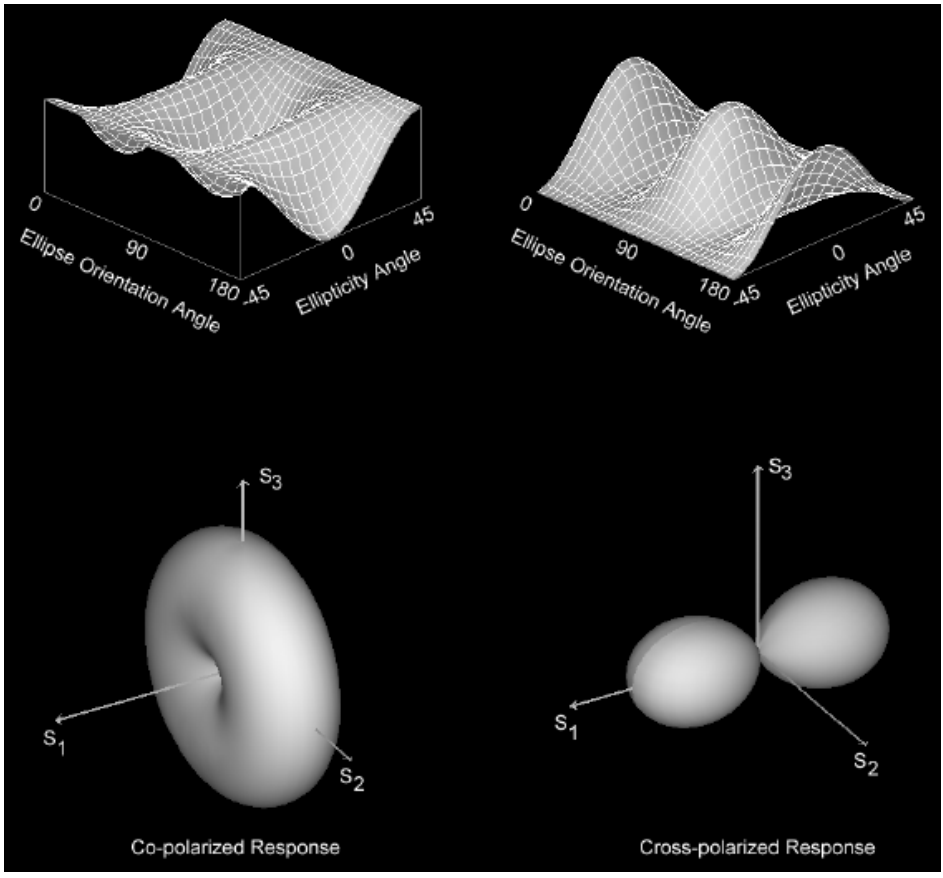

Fig. 2-11. Standard (top row) and three-dimensional (bottom row) polarization responses of a dihedral corner reflector rotated by an angle of 45 deg relative to the horizontal direction.

$$[\mathbf{C}] = |c_3|^2 \begin{pmatrix} 0 & 0 & 0 & 0 \\ 0 & 0 & 0 & 0 \\ 0 & 0 & 0 & 0 \\ 0 & 0 & 0 & 1 \end{pmatrix} \tag{2.4-14}$$

and

$$[\mathbf{M}] = \frac{|c_3|^2}{4} \begin{pmatrix} 1 & -1 & 0 & 0 \\ -1 & 1 & 0 & 0 \\ 0 & 0 & 0 & 0 \\ 0 & 0 & 0 & 0 \end{pmatrix}. \tag{2.4-15}$$

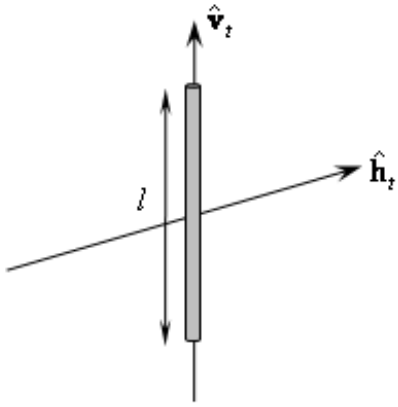

Fig. 2-12. A short, thin vertical conducting cylinder. The length of a cylinder is *l*.

The corresponding polarization responses are shown in Fig. 2-13. Note that both the co-polarized response is zero for HH polarization and the cross-polarized response is zero for VH polarization. This is the first example where both the co- and cross-polarized responses are zero for a given transmit polarization (horizontal polarization in this case). The reason for this is that when we transmit a horizontally polarized wave at this scatterer, there is no coupling to the cylinder and no scattered wave. Contrast this with the case of Fig. 2-11 for a horizontally polarized wave. The co-polarized response is zero, but the cross-polarized response is a not. This means that the scattered wave is non zero, but polarized orthogonally to the transmitted wave, and, hence, the maximum in the cross-polarized response.

Next, let us consider the case of a short, thin cylinder oriented at 45 deg from the vertical direction shown in Fig. 2-14. In this case, the scattering matrix is given by

$$[\mathbf{S}] = \frac{c_3}{2}\begin{pmatrix} 1 & -1 \\ -1 & 1 \end{pmatrix}, \tag{2.4-16}$$

where $c_3 = \dfrac{k_0^2 l^3}{6\left[\ln\left(4l/a\right)-1\right]}$ and a is the radius of a cylinder.

From Eq. (2.4-16), we can calculate the covariance matrix and the Stokes scattering operator as

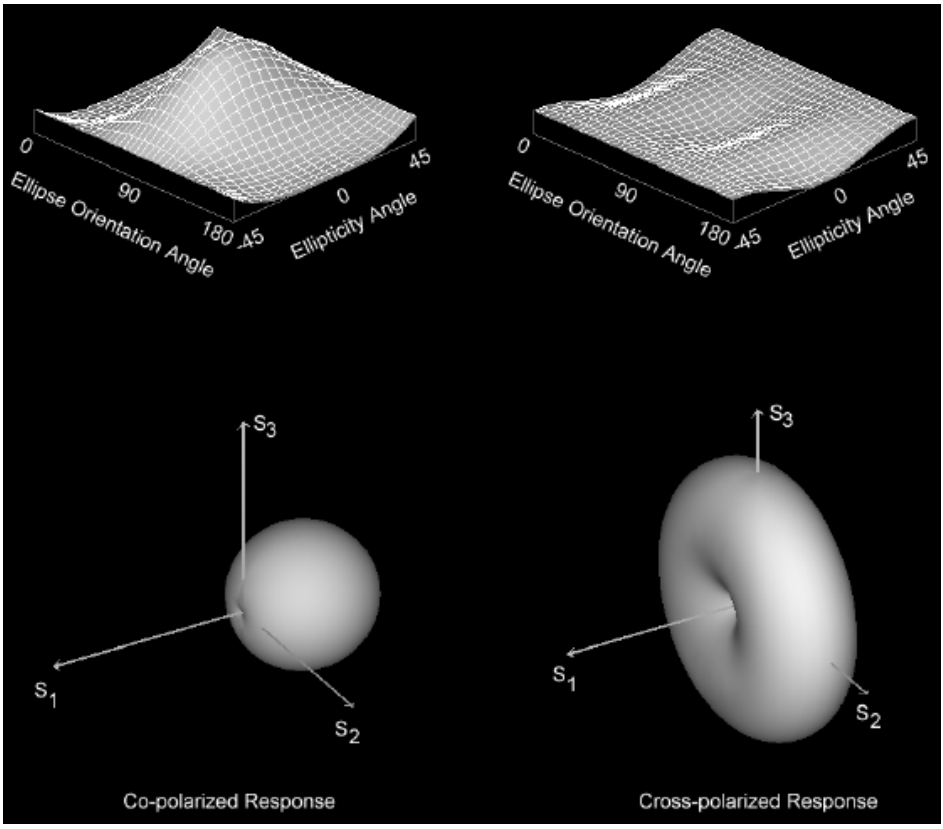

Fig. 2-13. The polarization responses of a short, thin, vertically oriented conducting cylinder.

$$[\mathbf{C}] = \frac{|c_3|^2}{4}\begin{pmatrix} 1 & -1 & -1 & 1 \\ -1 & 1 & 1 & -1 \\ -1 & 1 & 1 & -1 \\ 1 & -1 & -1 & 1 \end{pmatrix} \tag{2.4-17}$$

and

$$[\mathbf{M}] = \frac{|c_3|^2}{4}\begin{pmatrix} 1 & 0 & -1 & 0 \\ 0 & 0 & 0 & 0 \\ -1 & 0 & 1 & 0 \\ 0 & 0 & 0 & 0 \end{pmatrix}. \tag{2.4-18}$$

The corresponding polarization response is shown in Fig. 2-15. Note that the position of the maximum in the co-polarized responses has shifted to be at 45 deg linear polarization. This indicates that the polarization response is sensitive

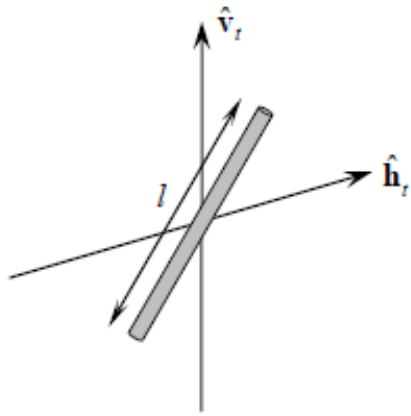

Fig. 2-14. A short, thin conducting cylinder oriented at 45 deg from the vertical direction. The length of a cylinder is *l*.

to the orientation of the short cylinder; we will exploit this fact when analyzing scattering from vegetation. Also, note that the cross-polarized response in Fig. 2-15 has the same shape as the co-polarized response in Fig. 2-10. This illustrates an important point: these polarization responses are not unique. In fact, these responses represent only a subset of the entire polarization space, and it is possible that more than one type of scatterer might have the same response. It would, therefore, be a mistake to consider the polarization responses as a unique way of identifying a specific type of scatterer.

Thus far, we have discussed only cases where the scatterer is characterized by a unique, single scattering matrix. In those cases, we have shown theoretically (we shall discuss this in more detail later) that the co-polarized and cross-polarized responses will each have at least one polarization for which the measured power goes to zero. When we analyze multi-looked data, however, we are working with the average power received from a collection of pixels. The composite polarization response can be thought of as the (properly normalized) sum of the individual polarization responses representing individual pixels. Unless all the individual responses have their null responses at exactly the same polarization, the composite signal will no longer have a null polarization. Instead, there might be some polarization for which the composite radar return is a minimum, but not zero.

To illustrate this further, let us consider the case of randomly oriented cylinders. This model has been used to describe scattering from randomly oriented tree branches that are thin compared to the radar wavelength. We shall start with a thin, conducting cylinder oriented at an angle α with respect to the

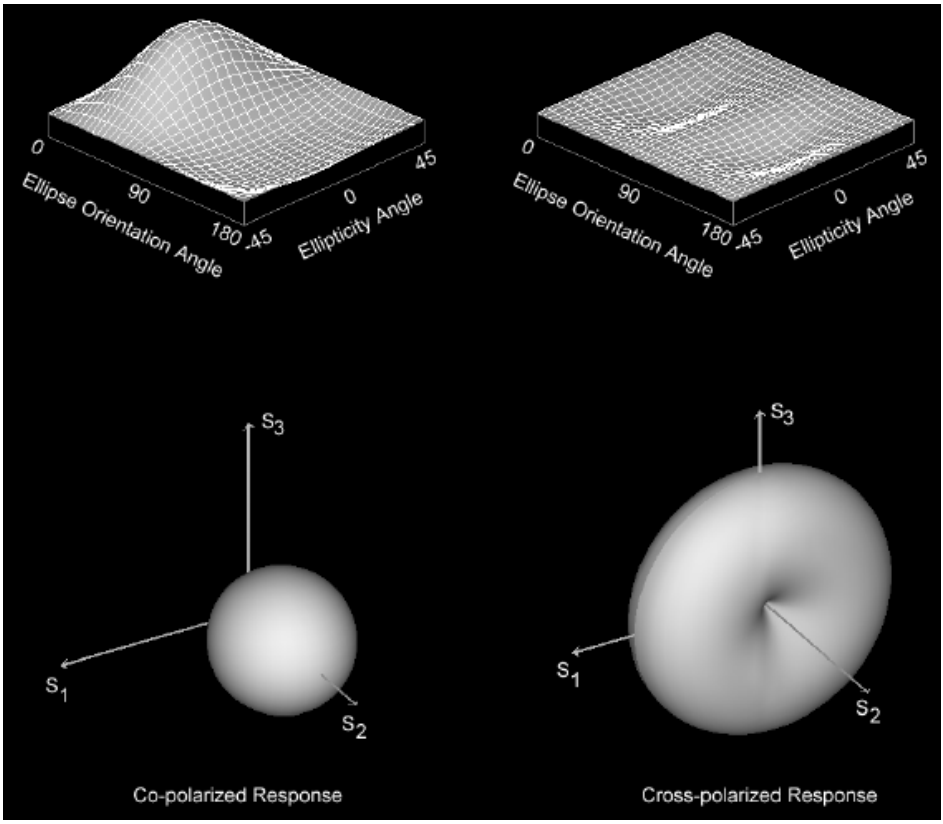

Fig. 2-15. The polarization response of a short, thin conducting cylinder oriented at 45 deg from the vertical direction. Note the difference between the responses in this figure and the responses shown in Fig. 2-13 for the vertically oriented cylinder.

vertical axis. The scattering matrix can be calculated by considering the rotation of the local coordinate axes defining the cylinder orientation, resulting in

$$\begin{bmatrix} S_{hh} & S_{hv} \\ S_{vh} & S_{vv} \end{bmatrix} = c_3 \begin{bmatrix} \cos\alpha & \sin\alpha \\ -\sin\alpha & \cos\alpha \end{bmatrix} \begin{bmatrix} 0 & 0 \\ 0 & 1 \end{bmatrix} \begin{bmatrix} \cos\alpha & -\sin\alpha \\ \sin\alpha & \cos\alpha \end{bmatrix}. \tag{2.4-19}$$

Here we assume that the cylinder lies in a plane that is orthogonal to the direction in which the radar waves travel. After straightforward matrix multiplications, the scattering matrix can be written as

$$\begin{bmatrix} S_{hh} & S_{hv} \\ S_{vh} & S_{vv} \end{bmatrix} = c_3 \begin{bmatrix} \sin^2\alpha & \sin\alpha\cos\alpha \\ \sin\alpha\cos\alpha & \cos^2\alpha \end{bmatrix}. \tag{2.4-20}$$

To illustrate the affect of randomness on the polarization response, we shall now analyze two different cases. In the first case, we assume that the cylinders are oriented uniformly randomly; i.e., we assume that α to be a random variable with a uniform distribution over [0,2π]. In this case, we find that

$$\begin{aligned}
&\left\langle S_{hh}S_{hh}^{*}\right\rangle = \frac{|c_3|^2}{2\pi}\int_0^{2\pi}\sin^4\alpha d\alpha = \frac{3}{8}|c_3|^2 \\
&\left\langle S_{vv}S_{vv}^{*}\right\rangle = \frac{|c_3|^2}{2\pi}\int_0^{2\pi}\cos^4\alpha d\alpha = \frac{3}{8}|c_3|^2 \\
&\left\langle S_{hv}S_{hv}^{*}\right\rangle = \left\langle S_{hh}S_{vv}^{*}\right\rangle = \left\langle S_{hv}S_{vh}^{*}\right\rangle = \left\langle S_{vh}S_{vh}^{*}\right\rangle = \frac{|c_3|^2}{2\pi}\int_0^{2\pi}\sin^2\alpha\cos^2\alpha d\alpha = \frac{1}{8}|c_3|^2 \\
&\left\langle S_{hh}S_{hv}^{*}\right\rangle = \left\langle S_{hv}S_{vv}^{*}\right\rangle = 0
\end{aligned} \quad . \qquad (2.4\text{-}21)$$

The covariance matrix for this case is

$$\left\langle[\mathbf{C}]\right\rangle = |c_3|^2\begin{pmatrix} 3/8 & 0 & 0 & 1/8 \\ 0 & 1/8 & 1/8 & 0 \\ 0 & 1/8 & 1/8 & 0 \\ 1/8 & 0 & 0 & 3/8 \end{pmatrix}. \qquad (2.4\text{-}22)$$

The Stokes scattering operator is

$$\left\langle[\mathbf{M}]\right\rangle = |c_3|^2\begin{pmatrix} 1/4 & 0 & 0 & 0 \\ 0 & 1/8 & 0 & 0 \\ 0 & 0 & 1/8 & 0 \\ 0 & 0 & 0 & 0 \end{pmatrix}. \qquad (2.4\text{-}23)$$

The polarization responses for this cloud of randomly oriented cylinders are shown in Fig. 2-16. Comparing these responses to those of the trihedral corner reflector, it is clear that they are similar except for the addition of a “pedestal” on which the responses sit. This “pedestal height” can be defined as the ratio of the minimum power in the response to the maximum power in the response. Using this definition, the pedestal height of a single scatterer will be zero, while the pedestal height for this example of the randomly oriented cylinders will be a non-zero value between 0 and 1. Therefore, the pedestal height can be used to infer the amount of randomness exhibited by multi-looked pixels.

To illustrate this point further, let us look at a second example involving the thin cylinders. Instead of assuming a uniform distribution in the angle α, we shall assume that the cylinders are mostly vertically oriented in a plane

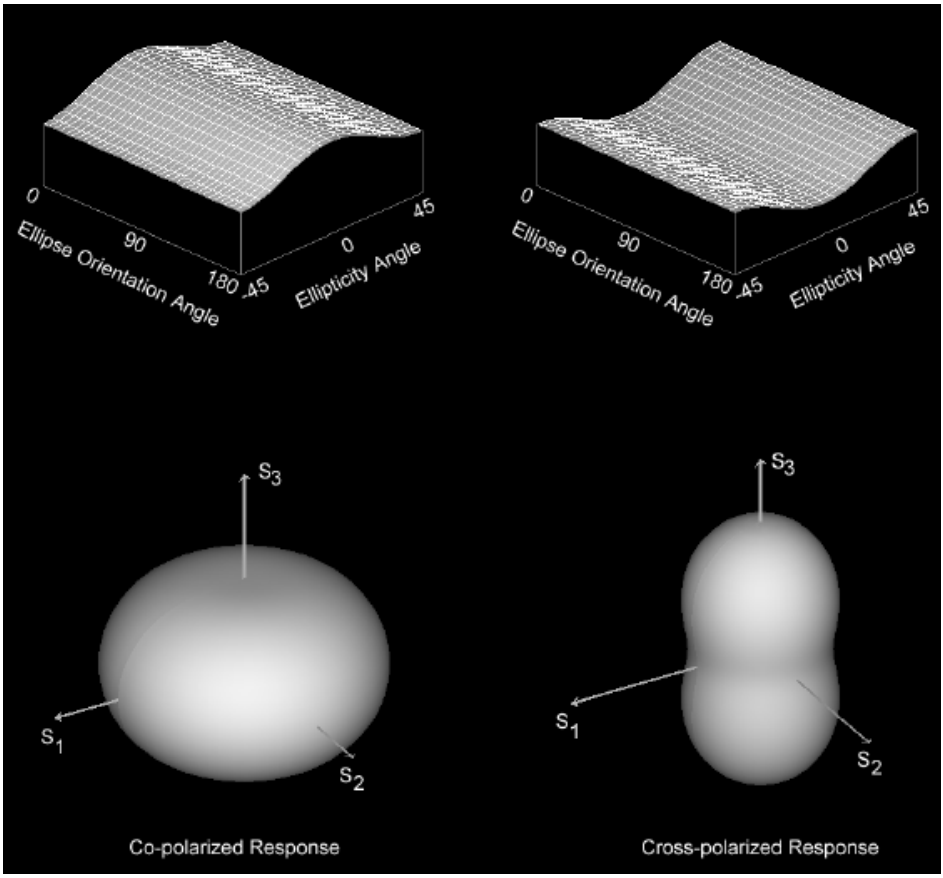

Fig. 2-16. Polarization responses of a cloud of thin conducting cylinders that are oriented uniformly randomly in a plane orthogonal to the radar look direction. Note that these shapes are similar to those shown for the trihedral corner reflector, except that the nulls in the responses have been replaced by non-zero minima.

orthogonal to the direction in which the radar signal is propagating. We shall assume the following probability density function for the cylinders:

$$p(\alpha) = \frac{1}{\pi}\cos^2\alpha; \quad 0 \le \alpha \le 2\pi \,. \tag{2.4-24}$$

This distribution has been used to describe scattering from vegetation, such as grass or wheat, which grows mostly vertically. Performing the averaging, we find

$$\begin{aligned}
&\left\langle S_{hh}S_{hh}^{*}\right\rangle = \frac{|c_3|^2}{2\pi}\int_0^{2\pi}\cos^2\alpha\sin^4\alpha\,d\alpha = \frac{1}{8}|c_3|^2 \\
&\left\langle S_{vv}S_{vv}^{*}\right\rangle = \frac{|c_3|^2}{2\pi}\int_0^{2\pi}\cos^6\alpha\,d\alpha = \frac{5}{8}|c_3|^2 \\
&\left\langle S_{hv}S_{hv}^{*}\right\rangle = \left\langle S_{hh}S_{vv}^{*}\right\rangle = \left\langle S_{hv}S_{vh}^{*}\right\rangle = \left\langle S_{vh}S_{vh}^{*}\right\rangle = \frac{|c_3|^2}{2\pi}\int_0^{2\pi}\sin^2\alpha\cos^4\alpha\,d\alpha = \frac{1}{8}|c_3|^2 \\
&\left\langle S_{hh}S_{hv}^{*}\right\rangle = \left\langle S_{hv}S_{vv}^{*}\right\rangle = 0
\end{aligned} \quad . \qquad (2.4\text{-}25)$$

The covariance matrix for this case is

$$\left\langle[\mathbf{C}]\right\rangle = |c_3|^2\begin{pmatrix} 1/8 & 0 & 0 & 1/8 \\ 0 & 1/8 & 1/8 & 0 \\ 0 & 1/8 & 1/8 & 0 \\ 1/8 & 0 & 0 & 5/8 \end{pmatrix}. \qquad (2.4\text{-}26)$$

The Stokes scattering operator is

$$\left\langle[\mathbf{M}]\right\rangle = |c_3|^2\begin{pmatrix} 1/4 & -1/8 & 0 & 0 \\ -1/8 & 1/8 & 0 & 0 \\ 0 & 0 & 1/8 & 0 \\ 0 & 0 & 0 & 0 \end{pmatrix}. \qquad (2.4\text{-}27)$$

The polarization responses for this cloud of randomly oriented cylinders are shown in Fig. 2-17. Compare the co-polarized response in the top left to that of a single, vertically oriented cylinder as shown in Fig. 2-13. These two responses are quite similar, with the exception that the response in Fig. 2-17 has a pedestal added to it. The relative height of this pedestal in the co-polarized response in Fig. 2-17 is 20 percent; however, the pedestal in Fig. 2-16 is 66 percent, clearly indicating the relationship between pedestal height and randomness.

So far, we have assumed that all the matrices are measured without any noise added to the measurements. In reality, of course, this is not the case. Before looking at the effect of system thermal noise on these responses, however, let us first examine the case of noise only. As mentioned in the previous section, scattering matrices are measured using two transmit pulses and two independent receiver channels.

Because measurements in a particular receiver are made at different times, and because the pulse repetition frequency is low enough so that the time between pulses (i.e., measurements) is much longer than the noise coherence time, the noise measurements in the four images corresponding to the scattering matrix

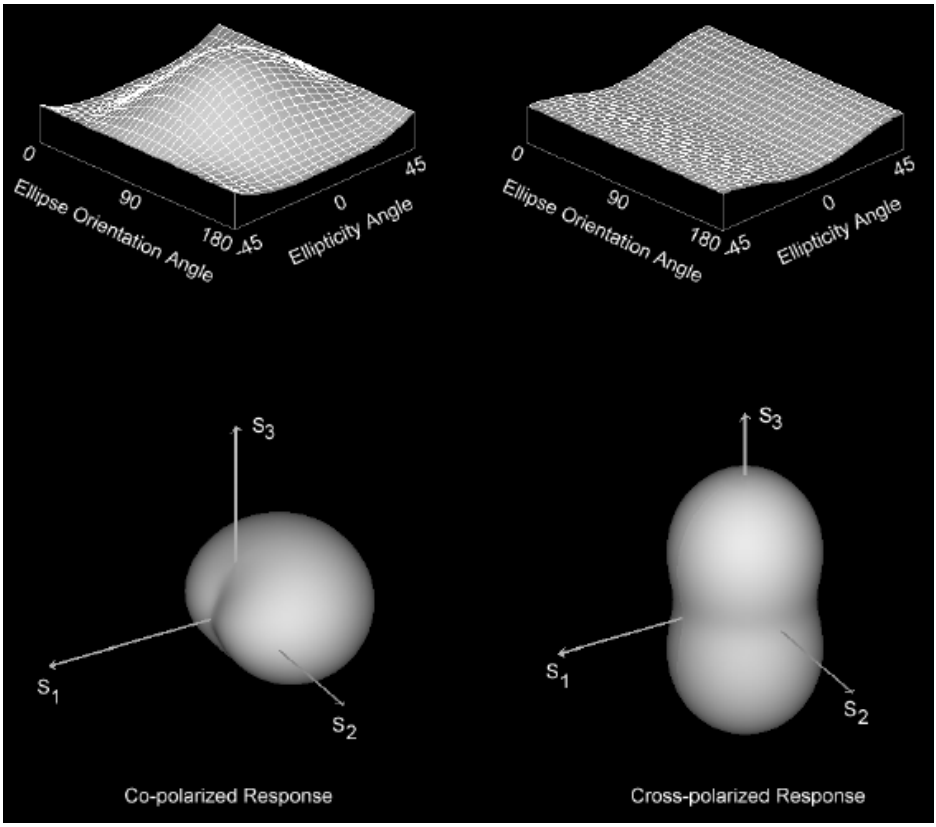

Fig. 2-17. Polarization responses for a cloud of dipoles with orientations according to the statistical distribution shown in Eq. (2.4-24). Note the similarity with the responses of a single, vertically oriented cylinder shown in Fig. 2-13, except for the addition of a pedestal. Also note the relative size of the pedestal in this figure, as compared to that of a uniform random orientation distribution shown in Fig. 2-16.

elements can be considered statistically independent. We shall further assume that the data, including the noise-only data, are well calibrated such that the channels are properly balanced in amplitude. In the absence of a return signal, after averaging, the covariance matrix will be an identity matrix, and the corresponding Stokes scattering operator will be

$$\langle [\mathbf{M}] \rangle = P_n \begin{pmatrix} 1 & 0 & 0 & 0 \\ 0 & 0 & 0 & 0 \\ 0 & 0 & 0 & 0 \\ 0 & 0 & 0 & 0 \end{pmatrix}. \tag{2.4-28}$$

This means, as expected, that the polarization response of a noise-only measurement is a constant value, independent of the transmit or receive

polarization. These polarization responses are shown in Fig. 2-18. Note that, in this case, the pedestal height is 100 percent.

In the backscatter case, reciprocity dictates that the two cross-polarized measurements should be identical. In practice, they differ because of the additive thermal noise in the receiver channels. As mentioned in the previous section, we can exploit the fact that the two cross-polarized measurements are made through different receivers and at different times, resulting in uncorrelated noise. If we average these two measurements before multi-looking, the noise power is effectively halved. Assuming that the noise power in each channel is P_n, the resulting noise power in the averaged cross-polarized channel will be

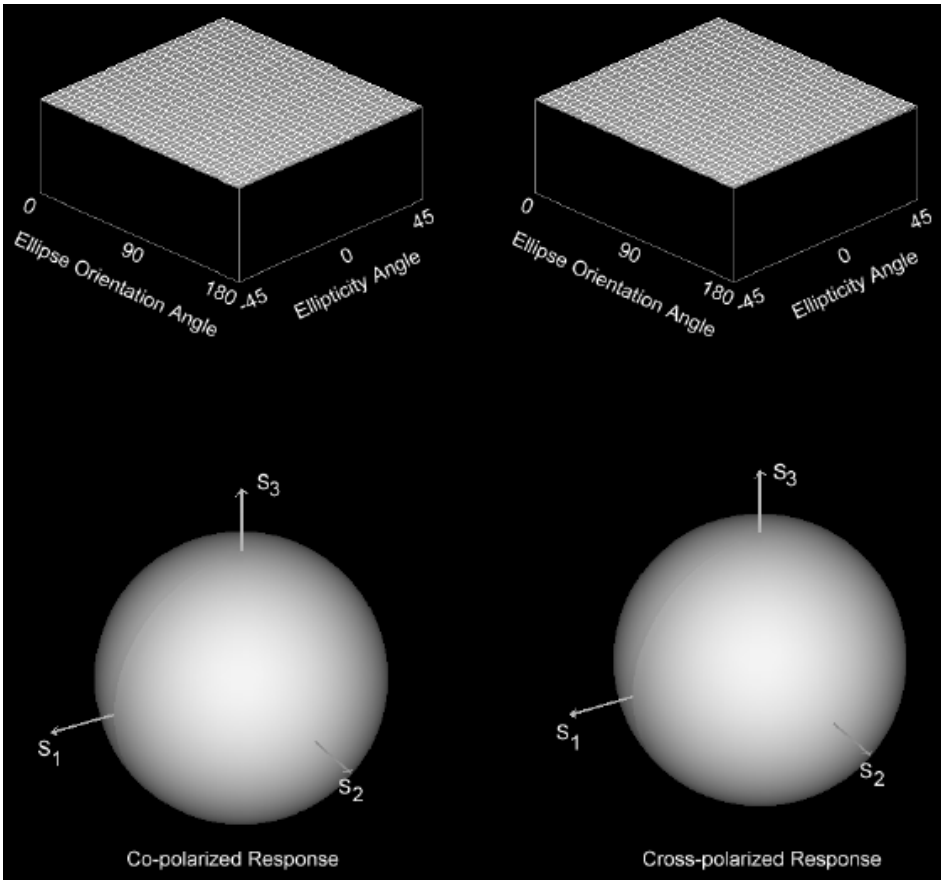

Fig. 2-18. The polarization responses of noise-only measurements when the noise power is identical in the two receiver channels. It is assumed that the cross-polarized channels are not averaged to increase the signal-to-noise ratio.

$$\begin{aligned}\left\langle S_{hv}S_{hv}^{*}\right\rangle &= \left\langle \frac{1}{4}\left(S_{hv}^{m}+S_{vh}^{m}\right)\left(S_{hv}^{m}+S_{vh}^{m}\right)^{*}\right\rangle \\ &= \left\langle \frac{1}{4}\left(S_{hv}^{m}\right)\left(S_{hv}^{m}\right)^{*}\right\rangle + \left\langle \frac{1}{4}\left(S_{hv}^{m}\right)\left(S_{vh}^{m}\right)^{*}\right\rangle + \left\langle \frac{1}{4}\left(S_{vh}^{m}\right)\left(S_{hv}^{m}\right)^{*}\right\rangle + \left\langle \frac{1}{4}\left(S_{vh}^{m}\right)\left(S_{vh}^{m}\right)^{*}\right\rangle \\ &= \frac{1}{4}P_n + 0 + 0 + \frac{1}{4}P_n \\ &= \frac{1}{2}P_n\end{aligned} . \tag{2.4-29}$$

The superscript m is added to indicate individual noise measurements. The second and third terms are zero because the noise in the two channels is uncorrelated. In this case, the covariance matrix is

$$\left\langle [\mathbf{C}]\right\rangle_N = P_n \begin{pmatrix} 1 & 0 & 0 & 0 \\ 0 & 1/2 & 1/2 & 0 \\ 0 & 1/2 & 1/2 & 0 \\ 0 & 0 & 0 & 1 \end{pmatrix} \tag{2.4-30}$$

and the Stokes scattering operator is

$$\left\langle [\mathbf{M}]\right\rangle_N = P_n \begin{pmatrix} 3/4 & 0 & 0 & 0 \\ 0 & 1/4 & 0 & 0 \\ 0 & 0 & 1/4 & 0 \\ 0 & 0 & 0 & 1/4 \end{pmatrix} . \tag{2.4-31}$$

The polarization responses of this case are shown in Fig. 2-19. Note that the pedestal is still 100 percent, but the cross-polarized responses are now less than the co-polarized ones.

To illustrate the effect of system noise on the polarization signatures, we note that the thermal noise and the radar signal are uncorrelated. The measured scattering matrix for each pixel can be written as

$$[\mathbf{S}]_m = [\mathbf{S}] + [\mathbf{N}] . \tag{2.4-32}$$

The first term on the right is the actual scattering matrix; the second term represents thermal noise in the system. Since the signal and noise are uncorrelated, the multi-looked covariance matrix is

$$\left\langle [\mathbf{C}]\right\rangle_m = \left\langle [\mathbf{C}]\right\rangle + \left\langle [\mathbf{C}]\right\rangle_N \tag{2.4-33}$$

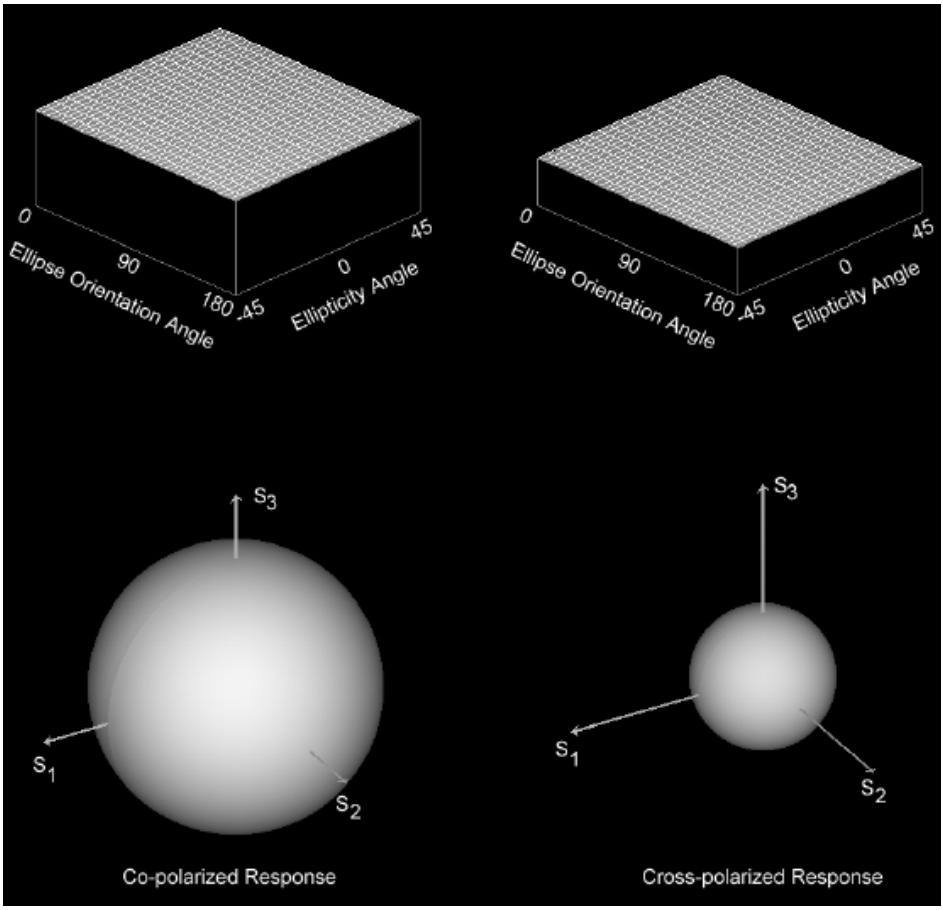

Fig. 2-19. Polarization responses of noise-only measurements when the cross-polarized channels are averaged before multi-looking to increase the signal-to-noise ratio in those channels.

and the multi-looked Stokes scattering operator is

$$\langle [\mathbf{M}] \rangle_m = \langle [\mathbf{M}] \rangle + \langle [\mathbf{M}] \rangle_N . \tag{2.4-34}$$

The noise matrices are the same as those in Eq. (2.4-30) and Eq. (2.4-31). The composite polarization response in the presence of noise will, therefore, be the sum of the actual scatterer response and that of the system noise. Since the system noise response is just a pedestal, the presence of the system noise will simply add a pedestal to the scatterer response. This is illustrated for the case of a vertically oriented thin cylinder with different amounts of thermal noise present in Fig. 2-20.

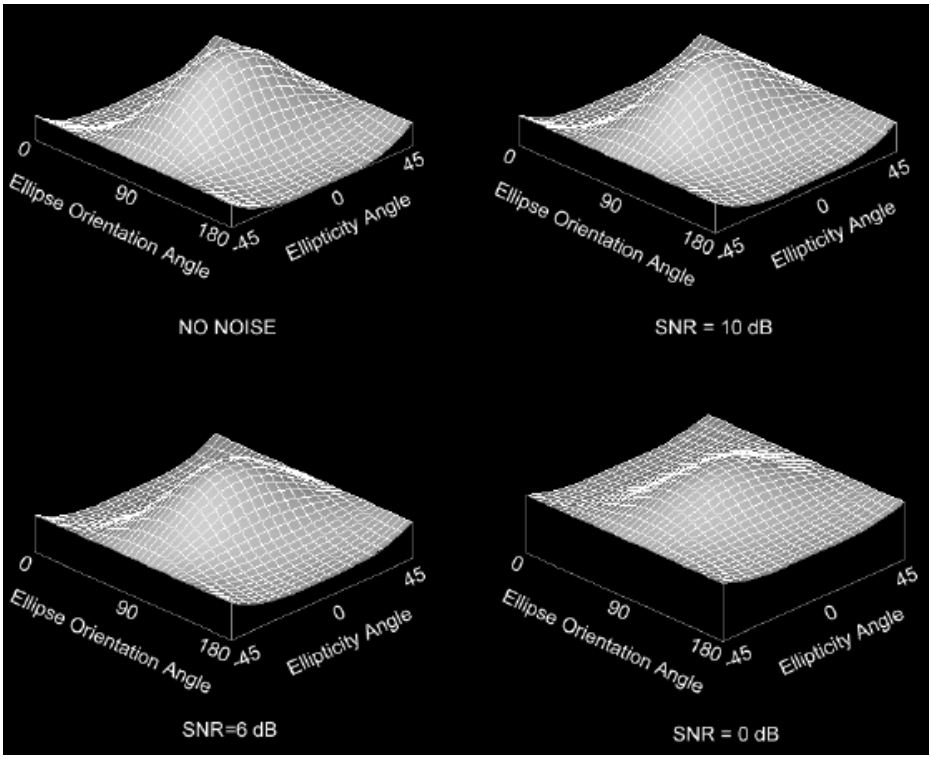

Fig. 2-20. Co-polarized responses of a thin conducting cylinder with various signal-to-noise ratios. Note the similarity of the SNR = 6dB response to that of the cosine squared random orientation shown in Fig. 2-17.

Note the similarity of the polarization response in the bottom left of Fig. 2-20 to that of the cloud of thin cylinders with a cosine squared distribution around the vertical direction. These figures illustrate an important point: the presence of a pedestal implies randomness, but the randomness can be due to many different causes. Care should, therefore, be exercised not to assume that the presence of a pedestal implies random orientation of scatterers without first verifying that there is an adequate signal-to-noise ratio (SNR) for this interpretation.

2.5 Optimum Polarizations

In the previous section, we introduced the concept of polarization responses as a way of visualizing the response of a scatterer, or a collection of scatterers after multi-looking. We shall now look at how to determine which polarization combination would optimize (i.e., either maximize or minimize) the received power from such a scatterer or collection of scatterers. We shall use the Stokes scattering operator representation of the scatterer for two reasons. First, it can be used to represent both a single scatterer or the ensemble average, or multi-

looked data. Second, it provides a simple, intuitive way of understanding how to optimize the received power by changing either the transmit or receive polarization. In the rest of this section, the matrix $[\mathbf{M}]$ will be used to mean either a single scatterer or a multi-looked average.

2.5.1 General (Bistatic) Case

This problem was first analyzed by Ioannidids and Hammers [11] in the context of maximizing radar signal strength in the presence of unwanted clutter. From Eq. (2.2-10) and Eq. (2.3-2), the received power can be written as

$$P = \mathbf{S}^{rec} \cdot [\mathbf{M}]\mathbf{S}^{tr}, \tag{2.5-1}$$

where $\mathbf{S}^{rec}$ and $\mathbf{S}^{tr}$ are the Stokes vectors representing the fully polarized waves of the receiving and transmitting antennas, respectively. Because these vectors represent fully polarized waves, each of these vectors has to satisfy Eq. (2.1-5). Therefore,

$$\mathbf{S} \cdot \begin{bmatrix} 1 & 0 & 0 & 0 \\ 0 & -1 & 0 & 0 \\ 0 & 0 & -1 & 0 \\ 0 & 0 & 0 & -1 \end{bmatrix} \mathbf{S} = 0 \,. \tag{2.5-2}$$

We can also write the Stokes scattering operator in the following form:

$$[\mathbf{M}] = \begin{bmatrix} m & \tilde{\mathbf{u}} \\ \mathbf{v} & \mathbf{Q} \end{bmatrix}, \tag{2.5-3}$$

with $\mathbf{u}$ and $\mathbf{v}$ three-dimensional real vectors and $\mathbf{Q}$ a 3 × 3 real matrix. The ~ sign indicates the transpose of the vector or matrix. Note that in the backscatter case, $\mathbf{u} = \mathbf{v}$ and $\mathbf{Q}$ is a symmetrical matrix. Now let us write the Stokes vectors of the antennas as

$$\mathbf{S}^{rec} = \begin{pmatrix} 1 \\ \mathbf{y} \end{pmatrix}; \quad \mathbf{S}^{tr} = \begin{pmatrix} 1 \\ \mathbf{x} \end{pmatrix}; \quad \mathbf{x} \cdot \mathbf{x} = 1; \quad \mathbf{y} \cdot \mathbf{y} = 1 \,. \tag{2.5-4}$$

Note that these vectors satisfy Eq. (2.5-2). Using Eq. (2.5-4) and Eq. (2.5-3) in Eq. (2.5-1), we find that

$$P = m + \mathbf{u} \cdot \mathbf{x} + \mathbf{v} \cdot \mathbf{y} + \mathbf{y} \cdot \mathbf{Q}\mathbf{x} \,. \tag{2.5-5}$$

This is the quantity we need to optimize, but subject to the constraints in Eq. (2.5-4). In the special case of co- and cross-polarized responses, either

$\mathbf{y} = \mathbf{x}$ or $\mathbf{y} = -\mathbf{x}$. To find the optima of P subject to the constraints in Eq. (2.5-4), we use the Lagrange multiplier method and construct the function

$$F = m + \mathbf{u}\cdot\mathbf{x} + \mathbf{v}\cdot\mathbf{y} + \mathbf{y}\cdot\mathbf{Q}\mathbf{x} + \frac{\lambda_x}{2}\left(1 - \mathbf{x}\cdot\mathbf{x}\right) + \frac{\lambda_y}{2}\left(1 - \mathbf{y}\cdot\mathbf{y}\right). \tag{2.5-6}$$

Let us first look at the receiving antenna polarization. The optimum polarizations are found by taking the derivatives of F:

$$\begin{aligned} \nabla_x F = 0 \;&\Rightarrow\; \lambda_x \mathbf{x} = \mathbf{u} + \tilde{\mathbf{Q}}\mathbf{y} \\ \nabla_y F = 0 \;&\Rightarrow\; \lambda_y \mathbf{y} = \mathbf{v} + \mathbf{Q}\mathbf{x} \end{aligned}. \tag{2.5-7}$$

The value of the Lagrange multiplier λ_y is found from the constraint in Eq. (2.5-4) that the magnitude of the vectors $\mathbf{y}$ and $\mathbf{x}$ must be 1. Using this constraint for the receiving antenna and the first equation in Eq. (2.5-7), we find that the optimum receive antenna polarization is given by

$$\mathbf{y} = \pm\frac{\mathbf{v} + \mathbf{Q}\mathbf{x}}{\sqrt{\left(\mathbf{v} + \mathbf{Q}\mathbf{x}\right)\cdot\left(\mathbf{v} + \mathbf{Q}\mathbf{x}\right)}}. \tag{2.5-8}$$

Let us examine this equation in more detail. The vector on the right is simply the polarized part of the vector that is the product of the Stokes scattering operator and the polarized part of the Stokes vector representing the transmitting antenna. Therefore, Eq. (2.5-8) simply states that the optimum receiving polarization is that Stokes vector that is either aligned with this vector or anti-podal to this vector on the Poincaré sphere. Further recall from our earlier discussion that orthogonal polarizations are anti-podal on the Poincaré sphere. Therefore, Eq. (2.5-8) simply states that the optimum receive polarizations for a given transmit polarization are those that either match the polarization of the incoming wave or are orthogonal to the polarization of the incoming wave.

From Eq. (2.5-7), we can now derive the following two expressions for the optimum transmit and receive antenna polarizations:

$$\begin{aligned} \left(\tilde{\mathbf{Q}}\mathbf{Q} - \lambda_x\lambda_y\mathbf{I}\right)\mathbf{x} &= -\left(\lambda_y\mathbf{u} + \tilde{\mathbf{Q}}\mathbf{v}\right) \\ \left(\mathbf{Q}\tilde{\mathbf{Q}} - \lambda_x\lambda_y\mathbf{I}\right)\mathbf{y} &= -\left(\lambda_y\mathbf{v} + \mathbf{Q}\mathbf{u}\right) \end{aligned}. \tag{2.5-9}$$

We can solve for the values of λ_x and λ_y using the constraint in Eq. (2.5-4) that the magnitude of the vectors $\mathbf{y}$ and $\mathbf{x}$ must be 1. This gives the following two expressions

$$\left|\left(\tilde{\mathbf{Q}}\mathbf{Q}-\lambda_x\lambda_y\mathbf{I}\right)^{-1}\left(\lambda_y\mathbf{u}+\tilde{\mathbf{Q}}\mathbf{v}\right)\right|=1$$
$$\left|\left(\mathbf{Q}\tilde{\mathbf{Q}}-\lambda_x\lambda_y\mathbf{I}\right)^{-1}\left(\lambda_y\mathbf{v}+\mathbf{Q}\mathbf{u}\right)\right|=1 \quad . \tag{2.5-10}$$

Once the values for λ_x and λ_y are known, we can use Eq. (2.5-9) to find the optimum polarization vectors.

These non-linear equations are not easy to solve explicitly. In practice, it is easier (and faster computationally) to use Eq. (2.5-8) in Eq. (2.5-5) to write the received power in the following form

$$P=m+\mathbf{u}\cdot\mathbf{x}\pm\sqrt{\left(\mathbf{v}+\mathbf{Q}\mathbf{x}\right)\cdot\left(\mathbf{v}+\mathbf{Q}\mathbf{x}\right)} \tag{2.5-11}$$

and to solve for the maxima or minima of Eq. (2.5-11) numerically, because the polarization response is a slowly varying function, as can be seen from the figures in the previous section. Once the optimum transmit polarizations have been identified, the optimum receive polarizations can be calculated using Eq. (2.5-8).

2.5.2 Backscatter (Monostatic) Case

So far, we have made no assumptions on the form of the Stokes scattering operator. In the special case of a monostatic radar, reciprocity dictates that the scattering matrix be symmetrical. In that case, the Stokes scattering operator is also symmetrical; i.e.,

$$\mathbf{u}=\mathbf{v};\quad \mathbf{Q}=\tilde{\mathbf{Q}}\,. \tag{2.5-12}$$

For this special case, the two expressions in Eq. (2.5-9) are identical, implying that the optimum receive polarization is related to the optimum transmit polarization by

$$\mathbf{y}=\pm\mathbf{x}\,. \tag{2.5-13}$$

In other words, the optimum values of the received power are found using co-polarized or cross-polarized antennas. We can then rewrite the power expression in Eq. (2.5-5) as follows

$$P_c=m+2\mathbf{u}\cdot\mathbf{x}+\mathbf{x}\cdot\mathbf{Q}\mathbf{x}$$
$$P_x=m-\mathbf{x}\cdot\mathbf{Q}\mathbf{x} \quad , \tag{2.5-14}$$

where the subscripts c and x refer to the co-polarized power and the cross-polarized power, respectively. We shall analyze the two cases separately. First,

consider the cross-polarized case. Solving for the optimum polarization vector subject to the constraint that the magnitude of this vector should be 1, gives the following expression

$$\mathbf{Q}\mathbf{x} = \lambda \mathbf{x} \,. \tag{2.5-15}$$

In other words, the optimum polarizations for the cross-polarized case are the normalized eigenvectors of the matrix $\mathbf{Q}$ and the optimum cross-polarized power values are

$$P_x = m - \lambda \,, \tag{2.5-16}$$

where λ represents the eigenvalues of the matrix $\mathbf{Q}$. Since $\mathbf{Q}$ is a symmetrical real matrix, all the eigenvectors are orthogonal to each other. This means that the optimum cross-polarized vectors are orthogonal when plotted on the Poincaré sphere. Note that the Stokes vectors, not the electric field vectors, are orthogonal.

The case of the co-polarized power is a bit more complicated. Taking the derivatives of the first equation in Eq. (2.5-14) subject to the constraint that the magnitude of the polarization vector should be 1 and setting the result equal to zero gives the following result

$$\left(\mathbf{Q} - \upsilon \mathbf{I}\right)\mathbf{x} = -\mathbf{u} \,. \tag{2.5-17}$$

As long as υ is not an eigenvalue of $\mathbf{Q}$, this equation has a unique solution:

$$\mathbf{x} = -\left(\mathbf{Q} - \upsilon \mathbf{I}\right)^{-1}\mathbf{u} \,. \tag{2.5-18}$$

In the special case where $\mathbf{u}$ is the null vector, the solutions to Eq. (2.5-17) are the normalized eigenvectors of $\mathbf{Q}$. In general, however, the optimum vectors $\mathbf{x}$ will not be eigenvectors of $\mathbf{Q}$. The values of υ are found from the constraint that the magnitude of $\mathbf{x}$ must be 1. The most intuitive solution is to write both $\mathbf{x}$ and $\mathbf{u}$ in the basis formed by the normalized eigenvectors of the matrix $\mathbf{Q}$. Since $\mathbf{Q}$ is a symmetrical matrix, these normalized eigenvectors are orthogonal and can be used as a basis to express these vectors. If we write $\mathbf{u}$ as

$$\mathbf{u} = b_1\hat{\mathbf{e}}_1 + b_2\hat{\mathbf{e}}_2 + b_3\hat{\mathbf{e}}_3 \,, \tag{2.5-19}$$

with $\hat{\mathbf{e}}_i \,; i = 1,2,3$ representing the normalized eigenvectors, we can solve for $\mathbf{x}$ from Eq. (2.5-17). The result is

$$\mathbf{x} = \frac{b_1}{(\upsilon - \lambda_1)}\hat{\mathbf{e}}_1 + \frac{b_2}{(\upsilon - \lambda_2)}\hat{\mathbf{e}}_2 + \frac{b_3}{(\upsilon - \lambda_3)}\hat{\mathbf{e}}_3, \tag{2.5-20}$$

where $\lambda_i; i = 1,2,3$ are the eigenvalues of $\mathbf{Q}$. The magnitude of this vector is

$$|\mathbf{x}| = \sqrt{\frac{b_1^2}{(\upsilon - \lambda_1)^2} + \frac{b_2^2}{(\upsilon - \lambda_2)^2} + \frac{b_3^2}{(\upsilon - \lambda_3)^2}}\,. \tag{2.5-21}$$

The values of υ are found by requiring that this magnitude be equal to 1. Solving for υ from this equation results in a sixth order polynomial in υ (van Zyl et al. [4]). The real valued roots of this polynomial are the optimum values of υ. The polynomial is

$$\upsilon^6 + d_1\upsilon^5 + d_2\upsilon^4 + d_3\upsilon^3 + d_4\upsilon^2 + d_5\upsilon + d_6 = 0, \tag{2.5-22}$$

with

$$\begin{aligned}
d_1 &= -2(\lambda_1 + \lambda_2 + \lambda_3) = -2m \\
d_2 &= (\lambda_1 + \lambda_2 + \lambda_3)^2 + 2(\lambda_1\lambda_2 + \lambda_1\lambda_3 + \lambda_2\lambda_3) - b_1 - b_2 - b_3 \\
d_3 &= -2\left[(\lambda_1 + \lambda_2 + \lambda_3)(\lambda_1\lambda_2 + \lambda_1\lambda_3 + \lambda_2\lambda_3) + \lambda_1\lambda_2\lambda_3\right] \\
&\quad + 2b_1(\lambda_2 + \lambda_3) + 2b_2(\lambda_1 + \lambda_3) + 2b_3(\lambda_1 + \lambda_2) \\
d_4 &= (\lambda_1\lambda_2 + \lambda_1\lambda_3 + \lambda_2\lambda_3)^2 + 2\lambda_1\lambda_2\lambda_3(\lambda_1 + \lambda_2 + \lambda_3) \\
&\quad - b_1\left(\lambda_2^2 + \lambda_3^2 + 4\lambda_2\lambda_3\right) - b_2\left(\lambda_1^2 + \lambda_3^2 + 4\lambda_1\lambda_3\right) - b_3\left(\lambda_1^2 + \lambda_2^2 + 4\lambda_1\lambda_2\right) \\
d_5 &= -2\lambda_1\lambda_2\lambda_3(\lambda_1\lambda_2 + \lambda_1\lambda_3 + \lambda_2\lambda_3) + 2b_1\lambda_2\lambda_3(\lambda_2 + \lambda_3) \\
&\quad + 2b_2\lambda_1\lambda_3(\lambda_1 + \lambda_3) + 2b_3\lambda_1\lambda_2(\lambda_1 + \lambda_2) \\
d_6 &= \lambda_1^2\lambda_2^2\lambda_3^2 - b_1\lambda_2^2\lambda_3^2 - b_2\lambda_1^2\lambda_3^2 - b_3\lambda_1^2\lambda_2^2
\end{aligned} \quad . \tag{2.5-23}$$

So how do we know that the polynomial in Eq. (2.5-22) has any real-valued roots? We can show that, in general, it will have at least two real-valued roots. This follows from the behavior of $|\mathbf{x}|$ as a function of υ, which is easiest seen from Eq. (2.5-21). As the value of υ approaches both $\pm\infty$, it is clear that $|\mathbf{x}| \to 0$. On the other hand, as the value of υ approaches any of the real-valued eigenvalues of the symmetrical matrix $\mathbf{Q}$, $|\mathbf{x}| \to \infty$. Therefore, there must be at least one value of υ between $-\infty$ and the smallest eigenvalue of $\mathbf{Q}$ for which $|\mathbf{x}| = 1$. Likewise, there must be at least one value of υ between the largest eigenvalue of $\mathbf{Q}$ and $\pm\infty$ and for which $|\mathbf{x}| = 1$. This proves that there will always be at least two real-valued roots to the polynomial in Eq. (2.5-22).

The one root will be less than the smallest eigenvalue of $\mathbf{Q}$, and the other will be larger than the largest eigenvalue of $\mathbf{Q}$.

2.5.3 Special Case: Single Scatterer in Backscatter (Monostatic) Case

Now let us consider the special case of the return from a single scatterer measured in the backscatter configuration. In this case, the scattering matrix $\mathbf{S}$ is symmetrical and there is a definite relationship between the elements of the matrix $\mathbf{Q}$. In fact, straightforward but tedious algebra shows that in this case, $\mathbf{Q}$ has three eigenvalues

$$\begin{aligned} \lambda_1 &= m \\ \lambda_2 &= \sqrt{\left(m-|\mathbf{u}|\right)\left(m+|\mathbf{u}|\right)} \geq 0 \quad . \\ \lambda_3 &= -\sqrt{\left(m-|\mathbf{u}|\right)\left(m+|\mathbf{u}|\right)} \leq 0 \end{aligned} \tag{2.5-24}$$

The normalized eigenvector corresponding to the first eigenvalue is $\pm\mathbf{u}/|\mathbf{u}|$. Using this eigenvalue in Eq. (2.5-14) shows that the vector $\pm\mathbf{u}/|\mathbf{u}|$ corresponds to a cross-polarized null. It also is a solution to Eq. (2.5-17) with

$$\upsilon = m \pm |\mathbf{u}| \,. \tag{2.5-25}$$

Using these in the top equation in Eq. (2.5-14) gives the two co-polarized powers of

$$P_c = 2\left(m \pm |\mathbf{u}|\right). \tag{2.5-26}$$

The plus sign corresponds to the maximum co-polarized power. Therefore, the polarization vector that maximizes the co-polarized power also results in a cross-polarized null. Also note from Eq. (2.5-26) that

$$P_{cs} = 2\left(m - |\mathbf{u}|\right) \geq 0 \Rightarrow m \geq |\mathbf{u}| \,. \tag{2.5-27}$$

As we shall see shortly, this co-polarized power represents the saddle point in the co-polarized response.

To find the vectors corresponding to the co-polarized minima, we define a normalized vector

$$\mathbf{x} = a\hat{\mathbf{e}}_1 + b\hat{\mathbf{e}}_3 \,, \tag{2.5-28}$$

where $\hat{\mathbf{e}}_1 = -\mathbf{u}/|\mathbf{u}|$ and $\hat{\mathbf{e}}_3$ are normalized eigenvectors of the matrix $\mathbf{Q}$ and a and b are real numbers. Since $\mathbf{Q}$ is a symmetrical matrix, these eigenvectors are orthogonal. Since $\mathbf{x}$ must have unit amplitude, it follows that we must require that

$$a^2 + b^2 = 1 . \tag{2.5-29}$$

The vector $\mathbf{x}$ must also be a solution to Eq. (2.5-17). If we use Eq. (2.5-28) in Eq. (2.5-17), we arrive at the following two equations:

$$\begin{aligned} \upsilon &= \lambda \\ a &= \frac{|\mathbf{u}|}{(m-\lambda)} \end{aligned} . \tag{2.5-30}$$

Here, λ is the eigenvalue corresponding to $\hat{\mathbf{e}}_3$. Combining the bottom line of Eq. (2.5-30) with Eq. (2.5-29) allows us to derive the value of b as

$$b = \pm\sqrt{1 - \frac{|\mathbf{u}|^2}{(m-\lambda)^2}} . \tag{2.5-31}$$

Using $\mathbf{x}$ with these values of a and b in the expression for the co-polarized power shows that the received power will be zero if λ corresponds to either λ_2 or λ_3 as given in Eq. (2.5-24). To decide which of the eigenvectors should be used in Eq. (2.5-28), we note that we can use Eq. (2.5-17) in the top line of Eq. (2.5-14) to write the co-polarized power as

$$P_{cn} = m + \mathbf{u}\cdot\mathbf{x} + \lambda = 0 \Rightarrow \lambda = -m - \mathbf{u}\cdot\mathbf{x} . \tag{2.5-32}$$

However,

$$-m - \mathbf{u}\cdot\mathbf{x} \le -m + |\mathbf{u}| = -\frac{1}{2}P_{cs} \le 0 \Rightarrow \lambda = \lambda_3 . \tag{2.5-33}$$

Therefore, we have two solutions that would lead to zero co-polarized power. These two are

$$\mathbf{x}_{n1} = -a\frac{\mathbf{u}}{|\mathbf{u}|} + \sqrt{1-a^2}\,\hat{\mathbf{e}}_3; \quad \mathbf{x}_{n1} = -a\frac{\mathbf{u}}{|\mathbf{u}|} - \sqrt{1-a^2}\,\hat{\mathbf{e}}_3 , \tag{2.5-34}$$

where

$$a = \frac{|\mathbf{u}|}{m + \sqrt{\left(m - |\mathbf{u}|\right)\left(m + |\mathbf{u}|\right)}} \,. \tag{2.5-35}$$

Equation (2.5-34) shows that the two co-polarized nulls and the co-polarized maximum and saddle point all lie in the same plane. Furthermore, the two co-polarized nulls are equal distances from the co-polarized saddle. This is easily proven by taking the dot products

$$-\frac{\mathbf{u}}{|\mathbf{u}|} \cdot \mathbf{x}_{n1} = -\frac{\mathbf{u}}{|\mathbf{u}|} \cdot \mathbf{x}_{n2} = a = \cos\alpha \,. \tag{2.5-36}$$

This is the famous polarization fork originally proven by Huynen in his landmark thesis (Huynen [12]).

Note that while the cross-polarized null polarization correspond to the co-polarized maximum polarization, the same is not true for the co-polarized null and the cross-polarized maximum. The co-polarized null polarizations are given in Eq. (2.5-34) and the cross-polarized maximum polarization vector is $\pm\hat{\mathbf{e}}_3$. The value of the maximum cross-polarized power is

$$P_{xm} = m + \sqrt{\left(m - |\mathbf{u}|\right)\left(m + |\mathbf{u}|\right)} \,. \tag{2.5-37}$$

Figure 2-21 shows these optimum polarizations on the Poincaré sphere.

2.5.4 Special Case: Multiple Scatterers with Reflection Symmetry

Here we shall consider the special case of the return from a group of scatterers with a special orientation distribution measured in the backscatter configuration. The orientation distribution is such that it is symmetrical about the vertical direction. In this case, it can be shown that

$$\left\langle S_{hv} S_{hh}^* \right\rangle = \left\langle S_{hv}^* S_{vv} \right\rangle = 0 \,. \tag{2.5-38}$$

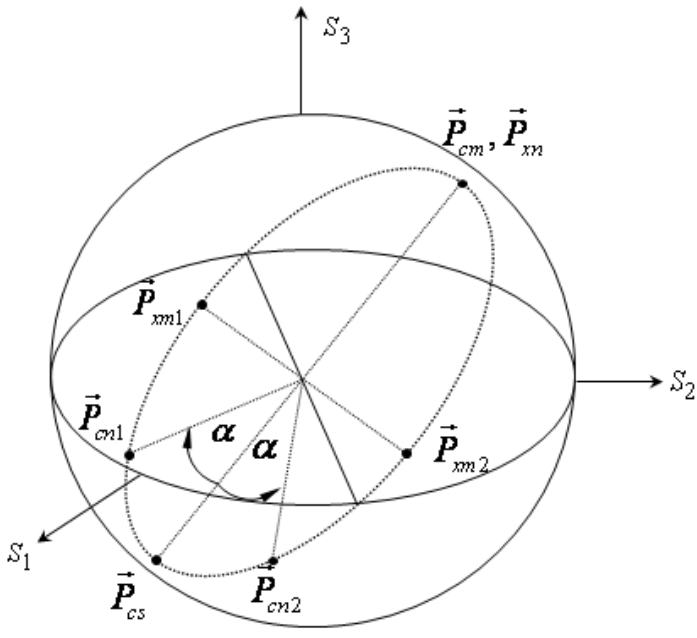

Fig. 2-21. The optimum polarizations plotted on the Poincaré sphere. The vectors corresponding to the co-polarized maximum, saddle point, and minima form the Huynen polarization fork. All these vectors lie in the same plane.

This leads to a special form of the Stokes scattering operator;

$$m = \frac{1}{4}\left\{\left\langle |S_{hh}|^2 \right\rangle + \left\langle |S_{vv}|^2 \right\rangle + 2\left\langle |S_{hv}|^2 \right\rangle\right\}$$

$$\mathbf{u} = \frac{1}{4}\left\{\left\langle |S_{hh}|^2 \right\rangle - \left\langle |S_{vv}|^2 \right\rangle\right\}\begin{bmatrix}1\\0\\0\end{bmatrix}$$

$$Q = \frac{1}{4}\begin{bmatrix} \left\langle |S_{hh}|^2 \right\rangle + \left\langle |S_{vv}|^2 \right\rangle - 2\left\langle |S_{hv}|^2 \right\rangle & 0 & 0 \\ 0 & 2\left\langle |S_{hv}|^2 \right\rangle + 2\,\mathrm{Re}\left\langle S_{hh}^* S_{vv} \right\rangle & 2\,\mathrm{Im}\left\langle S_{hh}^* S_{vv} \right\rangle \\ 0 & 2\,\mathrm{Im}\left\langle S_{hh}^* S_{vv} \right\rangle & 2\left\langle |S_{hv}|^2 \right\rangle - 2\,\mathrm{Re}\left\langle S_{hh}^* S_{vv} \right\rangle \end{bmatrix}$$

where $\langle x \rangle$ means the ensemble average of x. In this case, $\mathbf{Q}$ has three eigenvalues

$$\begin{aligned}\lambda_1 &= Q_{11} = m - \left\langle \left|S_{hv}\right|^2 \right\rangle \\ \lambda_2 &= \frac{1}{2}\left[\left\langle \left|S_{hv}\right|^2 \right\rangle + \left|\left\langle S_{hh}^* S_{vv} \right\rangle\right|\right] \\ \lambda_3 &= \frac{1}{2}\left[\left\langle \left|S_{hv}\right|^2 \right\rangle - \left|\left\langle S_{hh}^* S_{vv} \right\rangle\right|\right]\end{aligned} \tag{2.5-39}$$

The normalized eigenvector corresponding to the first eigenvalue is $\pm\mathbf{u}/|\mathbf{u}|$. Using this eigenvalue in Eq. (2.5-14) shows that the vector $\mathbf{u}/|\mathbf{u}|$ corresponds to a cross-polarized power value equal to $\left\langle \left|S_{hv}\right|^2 \right\rangle$. It also is a solution to Eq. (2.5-17) with

$$\upsilon = m - \left\langle \left|S_{hv}\right|^2 \right\rangle \pm |\mathbf{u}|. \tag{2.5-40}$$

Using these in the top equation in Eq. (2.5-14) gives the two co-polarized powers of

$$P_c = \left\langle \left|S_{hh}\right|^2 \right\rangle; \left\langle \left|S_{vv}\right|^2 \right\rangle. \tag{2.5-41}$$

To find the vectors corresponding to the co-polarized minima, we follow the same procedure as in the previous section and define a normalized vector

$$\mathbf{x} = a\hat{\mathbf{e}}_1 + b\hat{\mathbf{e}}_3, \tag{2.5-42}$$

where $\hat{\mathbf{e}}_1 = -\mathbf{u}/|\mathbf{u}|$ and $\hat{\mathbf{e}}_3$ are normalized eigenvectors of the matrix $\mathbf{Q}$ and a and b are real numbers. Since $\mathbf{Q}$ is a symmetrical matrix, these eigenvectors are orthogonal. In fact, the two eigenvectors corresponding to the second and third eigenvalues lie entirely in the plane containing the S_2 and S_3 axes of the Poincaré sphere. If $\mathrm{Im}\left\langle S_{hh}^* S_{vv} \right\rangle = 0$, these eigenvectors coincide with the S_2 and S_3 axes. Since $\mathbf{x}$ must have unit amplitude, it follows that we have to require that

$$a^2 + b^2 = 1. \tag{2.5-43}$$

The vector $\mathbf{x}$ must also be a solution to Eq. (2.5-17). If we use Eq. (2.5-28) in Eq. (2.5-17), we arrive at the following two equations:

$$\upsilon = \lambda$$

$$a = \frac{|\mathbf{u}|}{\left(m - \left\langle |S_{hv}|^2 \right\rangle - \lambda\right)}. \tag{2.5-44}$$

Here, λ is the eigenvalue corresponding to $\hat{\mathbf{e}}_3$. Combining the bottom line of Eq. (2.5-30) with Eq. (2.5-29) allows us to derive the value of b as

$$b = \pm\sqrt{1 - \frac{|\mathbf{u}|^2}{\left(m - \left\langle |S_{hv}|^2 \right\rangle - \lambda\right)^2}}. \tag{2.5-45}$$

Using $\mathbf{x}$ with these values of a and b in the expression for the co-polarized power shows that the received power will be

$$P_c = m + \lambda - \frac{|\mathbf{u}|^2}{\left(m - \left\langle |S_{hv}|^2 \right\rangle - \lambda\right)}. \tag{2.5-46}$$

The three values of the cross-polarized power are

$$P_x = \left\langle |S_{hv}|^2 \right\rangle; m - \frac{1}{2}\left\{\left\langle |S_{hv}|^2 \right\rangle \pm \left|\left\langle S_{hh}^* S_{vv} \right\rangle\right|\right\}. \tag{2.5-47}$$

Two of these values lie in the plane containing the S_2 and S_3 axes of the Poincaré sphere and one lies on the S_1 axis.

2.5.5 A Numerical Example

As an example of optimizing the power using independent transmit and receive antenna polarizations, let us consider the case of the randomly oriented cylinders from the previous section with a cosine squared distribution around the vertical direction. From Eq. (2.4-27), the normalized Stokes scattering operator have the following values

$$
\begin{aligned}
&m = 1 \\
&\tilde{\mathbf{u}} = \begin{pmatrix} -1/2 & 0 & 0 \end{pmatrix} \\
&\mathbf{v} = \mathbf{u} \\
&\mathbf{Q} = \begin{pmatrix} 1/2 & 0 & 0 \\ 0 & 1/2 & 0 \\ 0 & 0 & 0 \end{pmatrix}
\end{aligned}
\quad . \tag{2.5-48}
$$

In this case, the three eigenvalues of the matrix $\mathbf{Q}$ are 0, 1/2, and 1/2. The maximum cross-polarized return occurs for the polarization corresponding to the smallest eigenvalue; i.e., for circular polarizations. The minimum cross-polarized return occurs for the eigenvector corresponding to the largest eigenvalue, which, in this case, is any polarization that lies in the S_1-S_2 plane of the Poincaré sphere; i.e., any linear polarization.

The co-polarized solutions are simply the HH and VV returns, with the maximum occurring for VV and the minimum for HH. Note that for the case of $\lambda = 0$, we find from Eq. (2.5-45) and Eq. (2.5-48) that $b = 0$, which means that the minimum co-polarized power also coincides with the saddle point.

In this section, we concentrated on those polarization combinations that optimize (either maximizes or minimizes) the received power from a particular scatter or ensemble of scatterers. However, maximizing or minimizing the power from a single pixel, or even an area in an image, is of limited utility. This is best illustrated using the polarimetric L-band image of San Francisco acquired with the NASA/JPL AIRSAR system that we discussed earlier. Figure 2-22 shows the total power image (the trace of the covariance matrix, or the M_{11} element of the Stokes scattering operator) of this image with three co-polarized signatures of the ocean (top), an urban area (middle), and an area in Golden Gate Park (bottom). The maximum for the ocean occurs near VV. The other two signatures have their maxima near HH polarization. These two images are shown in Fig. 2-23. The HH image shows that the urban areas and park are bright relative to the ocean. The VV image shows the ocean to be bright relative to the urban areas. In image analysis, it is more common to require the contrast between two different areas to be maximized so as to be able to clearly identify similar areas. One of the earliest papers on this topic is the one by Ioannidis and Hammers [11] that reported on the optimum polarization to discriminate a target in the presence of clutter. We shall look at this problem in the next section.

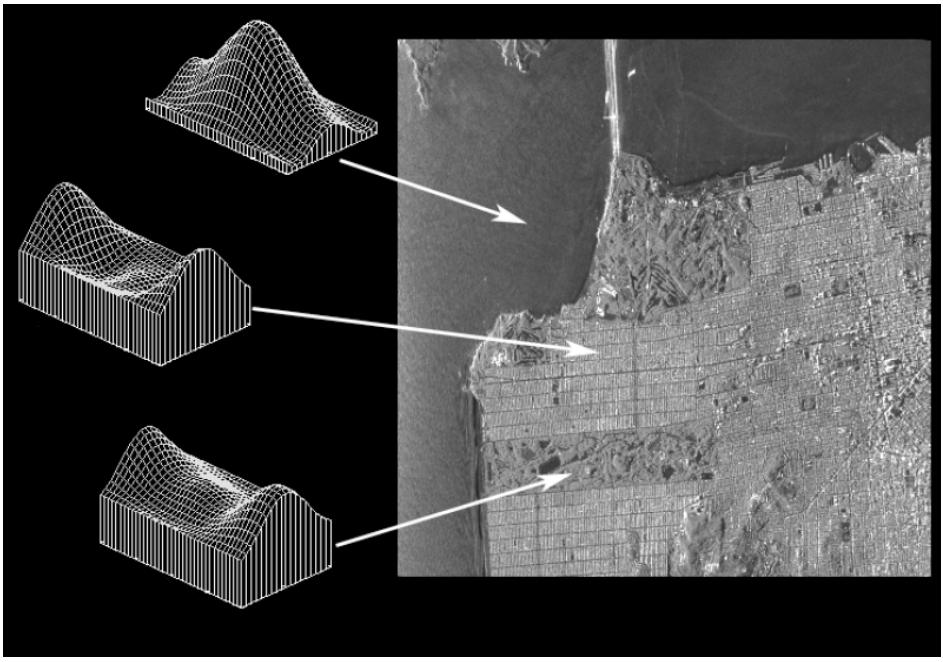

Fig. 2-22. An L-band total power image of San Francisco acquired with the NASA/JPL AIRSAR system. The three co-polarized signatures for the ocean, urban area, and Golden Gate Park are shown on the left.

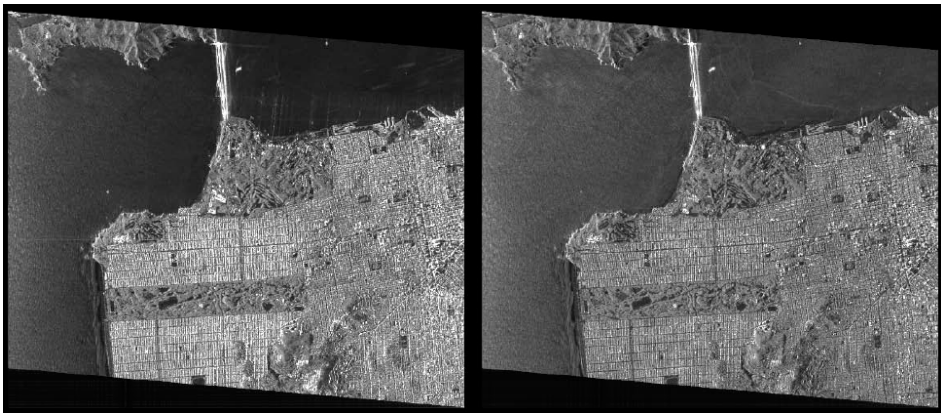

Fig. 2-23. HH polarized image (left) and VV polarized image (right) of San Francisco. The image on the left maximizes the power from the urban and park areas. The image on the right maximizes the power from the ocean. Note, however, that even though the power from the ocean is maximized in the image on the right, the contrast between the ocean and the urban areas is larger on the left.

2.6 Contrast Enhancement

Suppose we want to maximize or minimize the contrast between two areas in an image. We shall assume that each area is represented by an average Stokes scattering operator. The contrast can be written as

$$C_E = \frac{P_1}{P_2} = \frac{\mathbf{S}^{rec} \cdot \mathbf{M}_1 \mathbf{S}^{tr}}{\mathbf{S}^{rec} \cdot \mathbf{M}_2 \mathbf{S}^{tr}} = \frac{m_1 + \mathbf{u}_1 \cdot \mathbf{x} + \mathbf{v}_1 \cdot \mathbf{y} + \mathbf{y} \cdot \mathbf{Q}_1 \mathbf{x}}{m_2 + \mathbf{u}_2 \cdot \mathbf{x} + \mathbf{v}_2 \cdot \mathbf{y} + \mathbf{y} \cdot \mathbf{Q}_2 \mathbf{x}}, \tag{2.6-1}$$

where the subscripts 1 and 2 refer to the two areas. We now have to optimize this quantity subject to the constraints that the Stokes vectors have unit amplitude as shown in Eq. (2.5-4). To find the optimum values of the contrast function, we again use the Lagrange multiplier method as before and calculate the gradient with respect to $\mathbf{x}$ and $\mathbf{y}$. The optimum values are those for which the gradient is zero. This leads to the following two coupled equations:

$$\begin{aligned} \mathbf{y} &= \pm \frac{\mathbf{v}_1 + \mathbf{Q}_1 \mathbf{x} - C_E \left(\mathbf{v}_2 + \mathbf{Q}_2 \mathbf{x} \right)}{\left| \mathbf{v}_1 + \mathbf{Q}_1 \mathbf{x} - C_E \left(\mathbf{v}_2 + \mathbf{Q}_2 \mathbf{x} \right) \right|} \\ \mathbf{x} &= \pm \frac{\mathbf{u}_1 + \tilde{\mathbf{Q}}_1 \mathbf{y} - C_E \left(\mathbf{u}_2 + \tilde{\mathbf{Q}}_2 \mathbf{y} \right)}{\left| \mathbf{u}_1 + \tilde{\mathbf{Q}}_1 \mathbf{y} - C_E \left(\mathbf{u}_2 + \tilde{\mathbf{Q}}_2 \mathbf{y} \right) \right|} \end{aligned} . \tag{2.6-2}$$

The solution to these equations is a set of two non-linear equations in either $\mathbf{x}$ or $\mathbf{y}$ that is quite complex to solve. To provide more insight into the solution, a simpler approach is to consider the problem in two steps. First, we fix the transmit polarization and then derive the receive polarization that would optimize the contrast for that particular transmit polarization $\mathbf{x}$. For this, we introduce the shorthand notations:

$$\begin{aligned} S_{01} &= m_1 + \mathbf{u}_1 \cdot \mathbf{x} \\ \mathbf{s}_1 &= \mathbf{v}_1 + \mathbf{Q}_1 \mathbf{x} \\ S_{02} &= m_2 + \mathbf{u}_2 \cdot \mathbf{x} \\ \mathbf{s}_2 &= \mathbf{v}_2 + \mathbf{Q}_2 \mathbf{x} \end{aligned} . \tag{2.6-3}$$

It is then clear from the top line in Eq. (2.6-2) that we can write

$$\mathbf{y} = \frac{\mathbf{s}_1 - C_E \mathbf{s}_2}{\sqrt{\left(\mathbf{s}_1 - C_E \mathbf{s}_2 \right) \cdot \left(\mathbf{s}_1 - C_E \mathbf{s}_2 \right)}} . \tag{2.6-4}$$

Using this expression in the original expression for the contrast gives

$$C_E = \left\{ S_{01} + \frac{\mathbf{s}_1 \cdot \mathbf{s}_1 - C_E \mathbf{s}_1 \cdot \mathbf{s}_2}{\sqrt{(\mathbf{s}_1 - C_E \mathbf{s}_2) \cdot (\mathbf{s}_1 - C_E \mathbf{s}_2)}} \right\} \Big/ \left\{ S_{02} + \frac{\mathbf{s}_2 \cdot \mathbf{s}_1 - C_E \mathbf{s}_2 \cdot \mathbf{s}_2}{\sqrt{(\mathbf{s}_1 - C_E \mathbf{s}_2) \cdot (\mathbf{s}_1 - C_E \mathbf{s}_2)}} \right\}. \qquad (2.6\text{-}5)$$

The only unknown in this expression is the contrast ratio C_E. Rearranging terms leads to the following quadratic expression for this ratio

$$C_E^2 \left(S_{02}^2 - \mathbf{s}_2 \cdot \mathbf{s}_2 \right) - 2C_E \left(S_{01} S_{02} - \mathbf{s}_1 \cdot \mathbf{s}_2 \right) + \left(S_{01}^2 - \mathbf{s}_1 \cdot \mathbf{s}_1 \right) = 0 . \qquad (2.6\text{-}6)$$

The optimum contrast ratios are then

$$C_{\max}(\mathbf{x}) = \frac{S_{01} S_{02} - \mathbf{s}_1 \cdot \mathbf{s}_2}{S_{02}^2 - \mathbf{s}_2 \cdot \mathbf{s}_2} + \sqrt{\left(\frac{S_{01} S_{02} - \mathbf{s}_1 \cdot \mathbf{s}_2}{S_{02}^2 - \mathbf{s}_2 \cdot \mathbf{s}_2} \right)^2 - \frac{S_{01}^2 - \mathbf{s}_1 \cdot \mathbf{s}_1}{S_{02}^2 - \mathbf{s}_2 \cdot \mathbf{s}_2}} \qquad (2.6\text{-}7)$$

and

$$C_{\min}(\mathbf{x}) = \frac{S_{01} S_{02} - \mathbf{s}_1 \cdot \mathbf{s}_2}{S_{02}^2 - \mathbf{s}_2 \cdot \mathbf{s}_2} - \sqrt{\left(\frac{S_{01} S_{02} - \mathbf{s}_1 \cdot \mathbf{s}_2}{S_{02}^2 - \mathbf{s}_2 \cdot \mathbf{s}_2} \right)^2 - \frac{S_{01}^2 - \mathbf{s}_1 \cdot \mathbf{s}_1}{S_{02}^2 - \mathbf{s}_2 \cdot \mathbf{s}_2}} . \qquad (2.6\text{-}8)$$

These expressions are still quite complex to solve analytically for the $\mathbf{x}$ that optimizes either the maximum or minimum contrast ratio. A simpler approach, proposed by Dubois and van Zyl (1989) [13], is to solve for the maximum of Eq. (2.6-8) over all $\mathbf{x}$ numerically. Once this maximum ratio is found, the optimum receive polarization follows from the top equation in Eq. (2.6-2) to be

$$\mathbf{y} = \frac{\mathbf{s}_1 - C_{opt} \mathbf{s}_2}{\left| \mathbf{s}_1 - C_{opt} \mathbf{s}_2 \right|} . \qquad (2.6\text{-}9)$$

Note that these expressions turn out to be this complicated because we are insisting that the resulting Stokes vectors represent fully polarized waves; i.e., those of actual antennas. This, of course would be necessary if one wanted to implement a real radar system that operated with the optimum polarization combinations. However, for pure signal processing applications after data collection, one might want to relax this limitation. This approach was first reported by Swartz et al. [14] using the covariance approach for the backscatter case.

To illustrate the difference, let us assume that the two vectors $\mathbf{S}^{rec}$ and $\mathbf{S}^{tr}$ in Eq. (2.6-1) are simply 4-dimensional vectors. In that case, we solve for the optimum contrast by introducing (following Swartz et al. [14]) an artificial, but

general, constraint that the denominator of Eq. (2.6-1) should be equal to 1. The solution in this case then becomes

$$\begin{aligned} \mathbf{M}_1\mathbf{S}^{tr} &= \lambda_{tr}\mathbf{M}_2\mathbf{S}^{tr} \\ \tilde{\mathbf{M}}_1\mathbf{S}^{rec} &= \lambda_{rec}\tilde{\mathbf{M}}_2\mathbf{S}^{rec} \end{aligned}, \tag{2.6-10}$$

where λ_{tr} and λ_{rec} are the Lagrange multipliers. If the inverse of $\mathbf{M}_2$ exists, these expressions can be written as

$$\begin{aligned} \mathbf{M}_2^{-1}\mathbf{M}_1\mathbf{S}^{tr} &= \lambda_{tr}\mathbf{S}^{tr} \\ \tilde{\mathbf{M}}_2^{-1}\tilde{\mathbf{M}}_1\mathbf{S}^{rec} &= \lambda_{rec}\mathbf{S}^{rec} \end{aligned}, \tag{2.6-11}$$

Therefore, if we relax the requirement that the two vectors $\mathbf{S}^{rec}$ and $\mathbf{S}^{tr}$ represent fully polarized Stokes vectors, the solutions simply are the eigenvectors of $\mathbf{M}_2^{-1}\mathbf{M}_1$ and $\tilde{\mathbf{M}}_2^{-1}\tilde{\mathbf{M}}_1$. Note that, in the backscatter case, the Stokes scattering operators are symmetrical matrices and these two expressions become identical. This is also true for the solution to Eq. (2.6-2). If the inverse of $\mathbf{M}_2$ does not exist, we can rewrite Eq. (2.6-10) in a form that has the solution similar to Eq. (2.6-11), but with the roles of $\mathbf{M}_1$ and $\mathbf{M}_2$ interchanged.

2.6.1 Numerical Example

Consider the case of maximizing the contrast between the return from a dihedral corner reflector and that of a randomly oriented cloud of thin cylinders. In this case, the normalized Stokes scattering operators are

$$\mathbf{M}_1 = \begin{pmatrix} 1 & 0 & 0 & 0 \\ 0 & 1 & 0 & 0 \\ 0 & 0 & -1 & 0 \\ 0 & 0 & 0 & 1 \end{pmatrix}; \quad \mathbf{M}_2 = \begin{pmatrix} 1 & 0 & 0 & 0 \\ 0 & 1/2 & 0 & 0 \\ 0 & 0 & 1/2 & 0 \\ 0 & 0 & 0 & 0 \end{pmatrix}. \tag{2.6-12}$$

First we look at the case where we insist that the Stokes vectors represent fully polarized waves. Fig. 2-24 shows graphically the maximum and minimum contrast ratios for each transmit polarization. In each case, we performed the calculations that follow. For each of the transmit polarizations shown, we calculated the contrast ratio for all possible receive polarizations. We then found the maximum and minimum values and plotted those two values for that particular transmit polarization in these two figures. From Fig. 2-24 we see that the maximum contrast occurs for linear transmit polarizations that have

orientations of either 45 deg or 135 deg. The corresponding maximum contrast ratio is 4. Using this information, Eq. (2.6-9) gives the optimum receive polarization as either the co-polarized companion to the transmit polarization (in which case the contrast ratio is 0 [minimum]) or the cross-polarized companion (in which case the contrast ratio is 4, or a maximum).

This result is not unexpected. We know (see Fig. 2-10 and Fig. 2-16) that a dihedral corner reflector has its maximum cross-polarized return at 45 deg or 135 deg linear polarizations. At the same time, the linear polarizations are where the randomly oriented cylinders have their minimum in their cross-polarized return. This combination argues that the maximum contrast should then be at the 45 deg or 135 deg linear cross-polarized pair.

Next, let us consider the case where we do not insist that the solutions only be Stokes vectors representing fully polarized waves. In this case, the inverse of $\mathbf{M}_2$ does not exist. However, we can rewrite Eq. (2.6-10) by multiplying both sides by the inverse of $\mathbf{M}_1$ to give

$$\mathbf{M}_1^{-1}\mathbf{M}_2\mathbf{S} = \begin{bmatrix} 1 & 0 & 0 & 0 \\ 0 & 2 & 0 & 0 \\ 0 & 0 & -2 & 0 \\ 0 & 0 & 0 & 0 \end{bmatrix}\mathbf{S} = \lambda\mathbf{S}\,. \tag{2.6-13}$$

The eigenvalues are 2, 1, 0, and -2, and the corresponding four eigenvectors are the four principal dimensions of the vector $\mathbf{S}$. The Notice that this type of solution allows not only vectors that are not Stokes vectors, but also allows negative contrast ratios. The vector $\tilde{\mathbf{S}} = \begin{pmatrix} 0 & 1 & 0 & 0 \end{pmatrix}$ corresponds to the largest eigenvalue, but the largest contrast is actually achieved with the eigenvector $\tilde{\mathbf{S}} = \begin{pmatrix} 0 & 0 & 0 & \pm 1 \end{pmatrix}$ because, in this case, the denominator of the contrast is

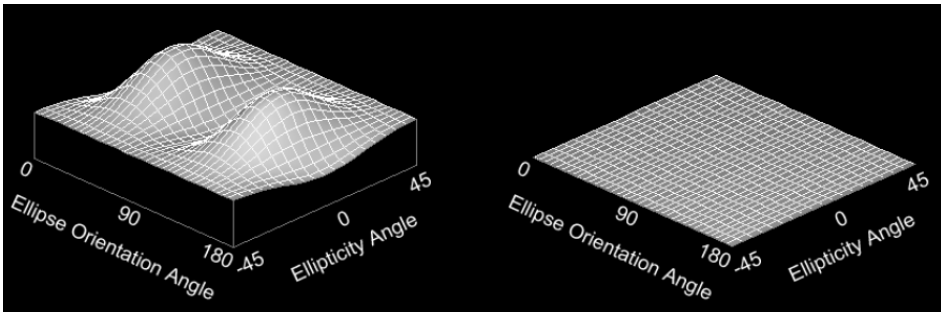

Fig. 2.24. The maximum (left) and minimum (right) contrast ratios calculated as a function of the transmit polarization orientation and ellipticity angles. The maximum contrast is achieved using a linear transmit polarization with an orientation of either 45 deg or 135 deg.

zero, theoretically allowing the contrast to approach infinity. Of course, in general, if there is any polarization combination that would zero out the power from the denominator, one could argue that the contrast ratio would be maximized. The problem with this approach is that the exact polarization combination at which the zero occurs might vary from one pixel in an image to the next, causing the result to be quite noisy.

2.6.2 Image Example

In the late 1980s, two different groups investigated the optimum polarizations to maximize the contrast between man-made structures (such as buildings) and natural terrain. Swartz et al. [14] used data from an area in the city of San Francisco to represent man-made structures and data from an area in Golden Gate Park for natural terrain. They found that the optimum polarizations were a transmitting antenna with parameters $(\psi_t, \chi_t) = (-41.3°, -6.44°)$ and a receiving antenna with parameters $(\psi_r, \chi_r) = (60.3°, 3.51°)$. Notice that these antennas are very nearly orthogonally polarized and close to the combination we derived in the previous section.

Dubois and van Zyl (1989) [13] made a more systematic study of the same problem, choosing many different pairs of areas and repeating the experiment at different incidence angles. They concluded that the optimum polarization varies little with the change in incidence angles and that a 45 deg cross-polarized pair provides the optimum contrast. They defined the polarization enhancement as the contrast calculated with normalized Stokes scattering operators and found the enhancement factor to be about 3 dB independent of the incidence angle and of the size of the image area used to characterize either class of scatterer. Furthermore, they found the same results if they used bare surfaces as the natural terrain.

Figure 2-25 illustrates this using the data from the NASA/JPL AIRSAR system that are shown in Fig. 2-23. Notice the excellent contrast between the urban areas and the vegetated Golden Gate Park, as well as the contrast between the urban areas and the ocean. Comparing to the image on the left in Fig. 2-23, we note some improvement in contrast between the urban area and the park. In fact, Swartz et al. [14] found that among the canonical polarization combinations, HH provided the best contrast, but was still about 2 dB less than what can be achieved with the optimum polarization combination.

Figure 2-26 shows the “image” using the non-physical polarization that theoretically zeros the power from a cloud of randomly oriented thin cylinders, as discussed in the previous section. This image, which is the M_{44} element of the Stokes scattering operator, shows the areas that are dominated by double

Fig. 2-25. Image of San Francisco, California, synthesized using a 45-deg linearly polarized antenna to transmit the signals and a 135-deg linearly polarized antenna to receive. Notice the increased contrast between the urban areas and the vegetated Golden Gate Park, as well as the contrast between the urban areas and the ocean.

reflections to be very bright, areas that are vegetated medium gray, and areas that have near specular scattering as very dark. To understand why this is the case, recall that for specular reflection the scattering matrix is the identity matrix. In that case, the M_{44} element of the normalized Stokes scattering operator is -1. The same element is zero for a randomly oriented cloud of thin cylinders and +1 for double reflections from a dihedral corner reflector.

Note, however, that this image is quite noisy, making it less useful than, for example, Fig. 2-25, for image-photo-interpretation purposes. It does, however, provide a simple check on whether a bright point in an image is so because it represents specular scattering or because it represents a double reflection resembling a dihedral corner reflector.

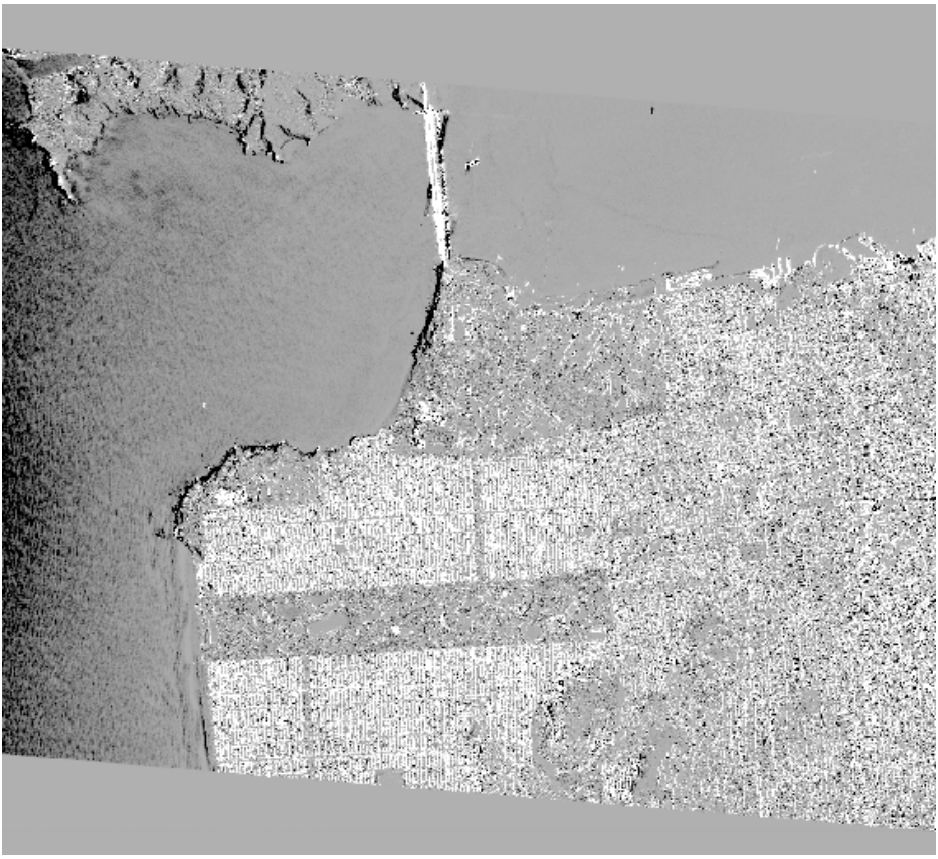

Fig. 2-26. "Image" of the M_{44} element of the Stokes scattering operator of San Francisco, California. Bright areas represent double reflections, while dark areas represent near-specular scattering. The image is quite noisy, reducing it utility for image-photo interpretation.

2.7 Summary

In this chapter, we introduced the basic principles of radar polarimetry. We introduced the important concepts of the various mathematical representations of scatterers and briefly reviewed the implementation of a radar polarimeter. We also discussed the concept of the polarization responses, and provided many examples illustrating this concept of visualizing the information contained in the polarization properties of a scatterer. Next, we looked at how to optimize the power received from a particular scatterer or group of scatterers by varying the polarization. We concluded with the case of using polarization to optimize the contrast between scatterers.

The discussion and examples presented in this chapter show the utility of polarization to extract more information regarding the properties of scatterers. In the rest of this book, we shall build upon these concepts and discuss more sophisticated analysis techniques to extract detailed geophysical information from polarimetric radar data.

References

[1] F. T. Ulaby and C. Elachi (Eds), *Radar Polarimetry for Geoscience Applications*, Artech House, Inc., Norwood, Massachusetts, 1990.

[2] E. M. Kennaugh, *Effects of the type of polarization on echo characteristics*, Report 389-9, Antenna Laboratory, Ohio State University, Columbus, Ohio, 1951.

[3] A. B. Kostinski and W. M. Boerner, "On Foundations of Radar Polarimetry," *IEEE Transactions on Antennas and Propagation*, vol. AP-34, pp. 1395-1404, 1986.

[4] J. J. van Zyl, H. A. Zebker, and C. Elachi, "Imaging Radar Polarization Signatures: Theory and Observation," *Radio Science*, vol. 22, pp. 529-543, 1987.

[5] H. A. Zebker, J. J. van Zyl, and D. N. Held, "Imaging Radar Polarimetry from Wave Synthesis," *Journal of Geophysical Research*, vol. 92, pp. 683-701, 1987.

[6] J. J. van Zyl, "On the Importance of Polarization in Radar Scattering Problems," Ph.D. Thesis, Caltech Antenna Laboratory Report No. 120, California Institute of Technology, Pasadena, California, 1985.

[7] J. J. van Zyl, C. H. Papas, and C. Elachi, "On the Optimum Polarizations of Incoherently Reflected Waves," *IEEE Transactions on Antennas and Propagation*, vol. AP-35, pp. 818-825, 1987.

[8] J. C. Souyris, P. Imbo, R. Fjortoft, S. Mingot, and J. S. Lee, "Compact Polarimetry Based on Symmetry Properties of Geophysical Media: the $\pi/4$ Mode," *IEEE Transactions on Geoscience and Remote Sensing*, vol. GE-43, pp. 634-646, 2005.

[9] R. K. Raney, "Hybrid-Polarity SAR Architecture," *IEEE Transactions on Geoscience and Remote Sensing*, vol. GE-45, pp. 3397-3404, 2007.

[10] A. P. Agrawal and W. M. Boerner, "Redevelopment of Kennaugh's Target Characteristic Polarization State Theory Using the Polarization Transformation Ratio for the Coherent Case," *IEEE Transactions on Geoscience and Remote Sensing*, vol. GE-27, pp. 2-14, 1988.

[11] G. A. Ioannidids and D. E. Hammers, "Optimum Antenna Polarizations for Target Discrimination in Clutter," *IEEE Transaction on Antennas and Propagation*, vol. AP-27, pp. 357-363, 1979.

[12] J. R. Huynen, *Phenomenological Theory of Radar Targets*, Ph.D. Dissertation, Drukkerij Bronder-Offset, N.V., Rotterdam, The Netherlands, 1970.

[13] P. C. Dubois and J. J. van Zyl, "Polarization Filtering of SAR data," *IGARSS '89 Digest*, vol. 3, pp. 1816-1819, 1989.

[14] A. A. Swartz, H. A. Yueh, J. A. Kong, L. M. Novak, and R. T. Shin, "Optimal polarizations for achieving maximum contrast in radar images," *Journal of Geophysical Research*, vol. 93, no. B12, pp. 15252-15260, 1988.